

1
2
3
4 **1 Seasonality and spatial heterogeneity of the surface ocean carbonate system in the**
5 **2 northwest European continental shelf**
6

7
8 3 Hartman, S.E.^a, Humphreys, M.P.^b, Kivimäe, C.^a, Woodward, E. M. S.^c, Kitidis, V.^c, McGrath,
9 4 T.^d, Hydes, D.J.¹, Greenwood, N.^e, Hull, T.^e, Ostle, C.^f, Pearce, D.J.^e, Sivyer, D.^e, Stewart,
10 5 B.M.^g, Walsham, P.^h, Painter, S.C.¹, McGovern, E.ⁱ, Harris, C.^c, Griffiths, A.^b, Smilenova, A.^b,
11 6 Clarke, J.^b, Davis, C.^j, Sanders, R.¹, Nightingale, P.^c

12
13 7 ^aNational Oceanography Centre, Southampton, UK

14
15 8 ^bOcean and Earth Science, University of Southampton, Southampton, UK

16
17 9 ^cPlymouth Marine Laboratory, Plymouth, UK

18
19 10 ^dNational University of Ireland, Galway, Ireland

20
21 11 ^eCentre for Environment Fisheries and Aquaculture Science (Cefas), Lowestoft, UK

22
23 12 ^fSir Alister Hardy Foundation for Ocean Science (SAHFOS), Plymouth, UK

24
25 13 ^gAgri-Food and Biosciences Institute (AFBI), Belfast, UK

26
27 14 ^hMarine Scotland Science (MSS), Aberdeen, UK.

28
29 15 ⁱThe Marine Institute, Galway, Ireland

30
31 16 ^jUniversity of Liverpool, Liverpool, UK

32
33 17

34
35 18 **Key words:**

36
37 19 Nutrients, carbonate chemistry, shelf seas

38
39 20

40
41 21 **Key message:**

42
43 22 We describe seasonal and regional variability in carbonate chemistry around the north-west
44 23 European shelf, from a large and unique 1.5 year dataset of biogeochemical sampling combined
45 24 with underway pCO₂ data. The data has improved understanding of carbonate chemistry in
46 25 relation to nutrient biogeochemistry, showing seasonal variations between the well-mixed
47 26 inner shelf and seasonally stratified outer shelf regions.
48
49
50

51
52 27

60
61
62 **28 Abstract**
63

64
65 29 In 2014-5 the UK NERC sponsored an 18 month long Shelf Sea Biogeochemistry research
66 30 programme which collected over 1500 nutrient and carbonate system samples across the NW
67 31 European Continental shelf, one of the largest continental shelves on the planet. This involved
68 32 the cooperation of 10 different Institutes and Universities, using 6 different vessels. Additional
69 33 carbon dioxide (CO₂) data were obtained from the underway systems on three of the research
70 34 vessels. Here, we present and discuss these data across 9 ecohydrodynamic regions, adapted
71 35 from those used by the EU Marine Strategy Framework Directive (MSFD). We observed strong
72 36 seasonal and regional variability in carbonate chemistry around the shelf in relation to nutrient
73 37 biogeochemistry. Whilst salinity increased (and alkalinity decreased) out from the near-shore
74 38 coastal waters offshore throughout the year nutrient concentrations varied with season. Spatial
75 39 and seasonal variations in the ratio of DIC to nitrate concentration were seen that could impact
76 40 carbon cycling. A decrease in nutrient concentrations and a pronounced under-saturation of
77 41 surface pCO₂ was evident in the spring in most regions, especially in the Celtic Sea. This
78 42 decrease was less pronounced in Liverpool Bay and to the North of Scotland, where nutrient
79 43 concentrations remained measurable throughout the year. The near-shore and relatively
80 44 shallow ecosystems such as the eastern English Channel and southern North Sea were
81 45 associated with a thermally driven increase in pCO₂ to above atmospheric levels in summer
82 46 and an associated decrease in pH. Non-thermal processes (such as mixing and the
83 47 remineralisation of organic material) dominated in winter in most regions but especially in the
84 48 northwest of Scotland and in Liverpool Bay. The large database collected will improve
85 49 understanding of carbonate chemistry over the North-Western European Shelf in relation to
86 50 nutrient biogeochemistry, particularly in the context of climate change and ocean acidification.
87
88
89
90
91
92
93
94
95
96
97
98
99
100

101 **51 1.0 Introduction**
102
103
104

105 53 Continental shelf seas are important net sinks of atmospheric CO₂, occupying only 7%
106 54 of the global sea surface area (Chen & Borges, 2009). However, there are considerable
107 55 uncertainties in the contributions of individual shelf seas to regional (and global) carbon
108 56 budgets (Borges, 2005). Continental shelves have high levels of biological activity due to cross
109 57 shelf and riverine nutrient supply, and to rapid organic matter recycling from the close pelagic-
110 58 benthic coupling on the shelf (Liu et al., 2010). The seawater partial pressure of CO₂ (pCO₂) is
111
112
113
114

119
120
121 59 controlled by seasonal changes in temperature and phytoplankton productivity (Zeebe & Wolf-
122 Gladrow, 2001). Additional factors such as coccolithophore calcification (Harley et al., 2010)
123 60
124 61 can influence seasonal variations in seawater pCO₂.

126 62 The northeast Atlantic continental shelf is a net CO₂ sink, of about -17 Tg C yr⁻¹
127 63 (compared with the global estimated shelf sink of -0.2 Pg C yr⁻¹; Laruelle et al., 2014) and thus
128 64 significant on both a regional and global basis as a hotspot of CO₂ uptake. It comprises both
130 65 well-mixed and stratified regions, which have different capacities to take up CO₂. Generally
132 66 the well mixed near-shore heterotrophic ecosystems act as sources of CO₂ to the atmosphere
134 67 and the seasonally stratified autotrophic continental shelf systems act as sinks of atmospheric
135 68 CO₂ (Borges, 2005; Chen & Borges, 2009). An example of the former is the southern North
137 69 Sea (Thomas et al., 2004) and the south western English Channel (Borges, 2005; Marrec et al.,
138 70 2013, 2015). An example of the latter is the seasonally stratified northern North Sea, which is
140 71 an order of magnitude stronger CO₂ sink than the well-mixed eastern English Channel (Thomas
141 72 et al., 2004, 2007). In the boundary between the off-shelf and on-shelf waters, a continuous
143 73 injection of nutrients can arise due to processes such as internal tides, internal waves, eddies
145 74 and slope current mixing, which can enhance productivity (Pingree, 1975; Garcia-Soto and
146 75 Pingree, 1998) and the potential CO₂ sink.

148 76 Monitoring the seawater total alkalinity (TA) and dissolved inorganic carbon (DIC),
149 77 along with its pCO₂, will help describe the oceanic carbonate system. The exact definition of
151 78 TA is complicated but it can be summarised as the stoichiometric sum of bases in solution
152 79 (Wolf-Gladrow et al., 2007). Many processes can influence TA such as benthic calcification
153 80 and dissolution, the growth of coccolithophore blooms (Harlay et al., 2010); the contribution
156 81 of organic matter (Koeve et al., 2012; Hoppe et al., 2012); changes in riverine input (Hydes &
157 82 Hartman, 2012) and nitrate uptake (Brewer & Goldman, 1976).

159 83 The anthropogenic increase in atmospheric CO₂ and uptake by seawater is driving a
160 84 decline in oceanic pH known as ocean acidification (OA) (Caldeira & Wickett, 2003; Doney
161 85 et al., 2009; Gattuso & Hansson, 2011). It is also important to measure nutrient concentrations
162 86 as an indication of potential primary production, as this will influence pCO₂ (and therefore
163 87 seawater pH) through the balance between photosynthesis and respiration.

167 88 The general features of the annual cycle of nutrient and plankton concentrations on the
168 89 northwest European shelf have been established for some time (Cushing, 1973; Johnston, 1973;
169 90 Gerlach, 1988; Nelissen & Stefels, 1988). Within the North Sea, the NERC North Sea
170 91 Programme in 1988-89, provided the first data set with sufficient information to allow seasonal

178
179
180 92 changes in nutrient concentrations and plankton biomass to be investigated quantitatively
181
182 93 (Howarth et al., 1996). Seasonal variation in carbonate chemistry has also been followed at
183
184 94 time series sites (eg: the L4 and Stonehaven sites during the 2008-2010 DEFRApH project,
185
186 95 Hydes et al., 2011) or through surveys around the NW European shelf (e.g. Thomas et al., 2004,
187
188 96 which was based on 4 surveys of the North Sea).

189 97 UK-SSB was established in 2014 to improve our understanding of carbon and nutrient
190
191 98 cycling within shelf seas. As part of the ‘CANDYFLOSS’ (Carbon and Nutrient DYnamics
192
193 99 and Fluxes Over Shelf Systems) component of UK-SSB, sampling was carried out across the
194
195 100 entire NW European continental shelf for DIC, TA and inorganic nutrients. The UK-SSB
196
197 101 sampling campaign was a large marine research community effort that started in January 2014
198
199 102 and continued for eighteen months, involving the cooperation of 10 institutes and universities
200
201 103 and 6 vessels. One aim of the present study was to increase the density and spatial coverage of
202
203 104 carbon and nutrient sampling across the entire NW European shelf, using the shelf wide
204
205 105 sampling component of the UK Shelf Sea Biogeochemistry research programme (UK-SSB,
206
207 106 <http://www.uk-ssb.org/>). Our aim was to describe how the biogeochemical variables are
208
209 107 distributed and interrelated on the shelf, both through the year and across 9 ecohydrodynamic
210
211 108 regions, adapted from those used by the EU Marine Strategy Framework Directive (MSFD).
212
213 109

210 110 **2.0 Materials and methods**

211 111 212 112 **2.1 Division of data into Ecohydrodynamic regions**

213 113 Ecohydrodynamic regions of the NW European Shelf are defined for reporting under
214
215 114 the EU Marine Strategy Framework Directive (MSFD). The regions have been adapted from
216
217 115 those defined in Charting Progress 2 (UKMMAS, 2010) and Bresnan et al., (2015), with the
218
219 116 addition of the Irish Continental Shelf and the Norwegian Trench. They are distinguished by
220
221 117 water depth (and seasonal stratification), proximity to the coast, riverine inputs (salinity) and
222
223 118 water temperature ranges. These regions and the sampling positions are shown in Figure 1.
224
225
226 119
227
228 120

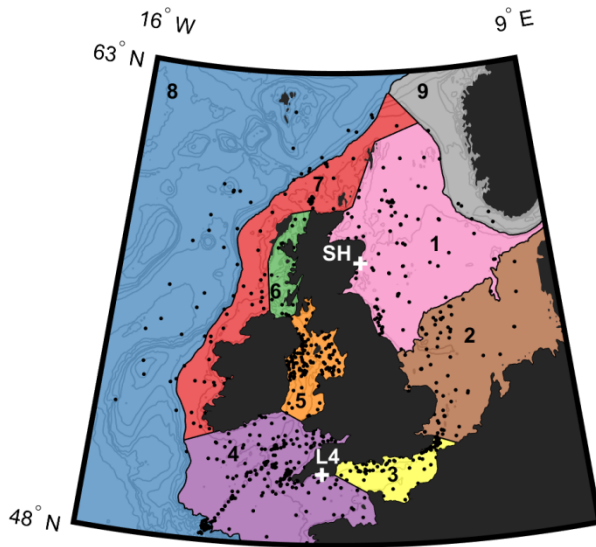


Figure 1: Map of the sampling positions (black dots) during UK-SSB (2014-2015). Coloured areas 1—9 show the UK ecohydrodynamic regions used for MSFD reporting (adapted from Bresnan et al., 2015 to now include Ireland and the Norwegian Trench and showing the 200m contour). White pluses show the time series sites SH (Stonehaven) and L4.

Complex tidal fronts and topography separate the well-mixed and seasonally stratified waters across the shelf. This will strongly influence the biogeochemical dynamics of the area (as shown by Simpson & Hunter, 1974). The biogeochemical divide along the 50m contour separates the seasonally stratified northern North Sea (region 1) from the shallower, well-mixed southern North Sea (region 2). The North Sea is influenced by the Atlantic Ocean to the North (Huthnance et al., 1997) and by riverine input, especially to the south (Hydes et al., 1999; Bresnan et al., 2015). The northern North Sea acts as a down-welling system (Huthnance et al., 2009). In the southern North Sea the entire water column remains well mixed throughout the year, likewise the eastern Channel (region 3) has shallow (0-100m) and tidally well mixed waters. The deeper western Channel and Celtic Sea (region 4) has strong seasonal stratification with Atlantic influences in the Celtic Sea (Pingree, 1993; Simpson & Hunter, 1974). The relatively shallow and enclosed Irish Sea and especially Liverpool Bay (region 5) have a high influence of fresh water input (Hydes & Hartman, 2012; Greenwood et al., 2011).

Waters west of Scotland and the Minches (region 6) are made up of North Atlantic Ocean waters and form part of the continental shelf current but are modified by coastal

296
297
298
299
300
301
302
303
304
305
306
307
308
309
310
311
312
313
314
315
316
317
318
319
320
321
322
323
324
325
326
327
328
329
330
331
332
333
334
335
336
337
338
339
340
341
342
343
344
345
346
347
348
349
350
351
352
353
354

142 influences (Bresnan et al, 2015). The Scottish and Irish continental shelf (region 7) are
143 characterised by seasonal stratification and, as defined here, have a western limit of the 200m
144 depth contour. This region is influenced both by exchanges with the North Atlantic deep water
145 and by water flowing from the south in the shelf edge current (Pingree, 1993; Huthnance, 1995
&1997; Hydes et al 2004). The deep-sea waters beyond the 200m contour are oceanic in origin
147 and the Atlantic Approaches (region 8) encompasses the Rockall Trough and the
148 Faeroe/Shetland Channel. The Norwegian Trench (region 9) is the main outflow path for water
149 leaving the North Sea, and it is permanently stratified (Van Leeuwen et al., 2015).

151 **2.2 Sample collection**

152 Between January 2014 and August 2015, multiple organisations collected samples from
153 the underway water supply of their vessels on a daily basis whenever they were at sea around
154 the NW European shelf (Figure 1). Data were obtained from RRS *Discovery* (8 cruises), RRS
155 *James Cook* (1 cruise), RV *Cefas Endeavour* (34 cruises), RV *Celtic Explorer* (6 cruises), RV
156 *Scotia* (7 cruises), RV *Corystes* (15 cruises), with additional samples from the fixed point
157 monitoring sites Stonehaven in the North Sea and L4 in the English Channel (Figure 1). All
158 data are available from BODC <http://www.uk-ssb.org/data/> and as listed in the references from
159 Humphreys et al., 2017 (a-h).

160 On approximately 1500 occasions, surface samples were collected from the underway
161 seawater supply (nominal 5m depth). For DIC and TA analysis the samples were collected into
162 borosilicate glass bottles (preserved with 0.05 ml saturated mercuric chloride solution
163 following Dickson et al., 2007), and the nutrient samples were filtered and frozen. At the time
164 of sampling the temperature and salinity was recorded from the underway sensors. Additional
165 near surface (0-20 m) samples were taken using a rosette sampler on the UK-SSB cruises in
166 the Celtic Sea, on the RV *Cefas Endeavour* and on a supporting cruise to the Hebrides Shelf
167 (Painter et al., 2016; Hartman et al., 2017).

168 **2.3 Chemical analysis**

170 DIC and TA were mostly (>95%) measured using VINDTA 3C (Marianda, Germany)
171 instruments in our shore based laboratory in Southampton. DIC analysis on the VINDTA
172 involves reaction with 10% phosphoric acid, which converts DIC to CO₂ gas. This is carried

355
356
357 173 by nitrogen into the coulometer cell where it reacts with monoethanolamine forming a titratable
358
359 174 acid, which causes fading of the blue indicator. Responding to the colour change, an electrical
360
361 175 current generates base to remove the acid and restore the indicator to the original colour. The
362
363 176 amount of CO₂ can be estimated from the total current required (corrected for a blank), and
364
365 177 DIC concentration can then be calculated given the sample volume. TA was measured by
366
367 178 titration with hydrochloric acid (HCl ~0.10 mol l⁻¹) using an open cell procedure, with a pH
368
369 180 half-cell electrode (glass bodied Orion 8101SC, Ross, USA) and an Ag/AgCl reference
370
371 181 electrode (model 6.0729.100, Metrohm, Switzerland). A modified Gran plot approach was used
372
373 182 to calculate TA (Humphreys, 2015). Approximately 5% of the DIC and TA measurements were
374
375 183 conducted using the Apollo SciTech (USA) DIC Analyzer (AS-C3) and Total Alkalinity
376
377 184 Titrator (AS-ALK2). The AS-C3 functions similarly to the VINDTA 3C except that the final
378
379 185 CO₂ measurement is by infrared absorbance (LI-COR). The AS-ALK2 performs a
380
381 186 potentiometric titration with 0.1M HCl to determine the TA.

382
383 186 In order to calibrate the results, seawater reference material (RM) obtained from A.G.
384
385 187 Dickson (Scripps Institution of Oceanography, USA) were analysed each day (Dickson et al.,
386
387 188 2003). Precision was assessed through repeated measurements of pooled seawater samples
388
389 189 (n>3) before each batch of sample analysis. The 1σ precision for the whole dataset was
390
391 190 estimated as ±2.6 μmol kg⁻¹ for DIC and ±2.7 μmol kg⁻¹ for TA for VINDTA measurements.
392
393 191 For the Apollo measurements, precision was estimated as ±4.0 μmol kg⁻¹ and ±3.9 μmol kg⁻¹
394
395 192 for DIC and TA respectively (Humphreys et al., 2017, this issue).

396
397 193 During the SSB shelf wide sampling, underway pCO₂ was measured on-board the RV
398
399 194 *Cefas Endeavour* and on the NERC research vessel RRS *Discovery* using PML-Dartcom
400
401 195 systems (Kitidis et al., 2012). Briefly, this comprises of a vented ‘showerhead’ equilibrator,
402
403 196 Peltier cooler for partial drying of the equilibrated gas stream, non-dispersive infrared detection
404
405 197 (Licor; LI-840) and associated mechanical/electronic hardware. The system was calibrated
406
407 198 against three reference gases (BOC Gases, UK; nominal concentrations 250, 380 and 450 ppmv
408
409 199 CO₂ in synthetic air mixtures; changing from 450ppm to 600ppm on the RV *Cefas Endeavour*
410
411 200 from November 2014) which were referenced against primary reference gases (National
412
413 201 Oceanic and Atmospheric Administration, 244.9 and 444.4 ppm CO₂). A recent at-sea inter-
414
415 202 comparison with a similar but independent system, along with other carbonate observations,
416
417 203 found the system was precise to within ±4 μatm (Ribas-Ribas et al., 2014). The atmospheric
418
419 204 pCO₂ was calculated from monthly averaged pCO₂ measured at Mace Head (53.33° N, 9.90°
420
421 205 W) (Humphreys et al., this issue).

414
415
416 206 Inorganic nutrients were analysed using a ‘Bran and Luebbe AA3’ segmented flow
417
418 207 colorimetric nutrient auto-analyser. The analytical methods were phosphate and silicate using
419
420 208 Kirkwood (1989) and nitrate (plus nitrite) with Brewer and Riley (1965) methods. The standard
421
422 209 deviation for duplicate measurements was within 2% and quality was assured through daily
423
424 210 use of certified reference materials provided by KANSO (Japan). Sampling protocols and
425
426 211 methodologies were carried out where possible according to the GO-SHIP nutrient analytical
427
428 212 procedures manual (Hydes et al., 2010) including assessment of detection limits (eg: 0.1 μmol
429
430 213 kg^{-1} for nitrate).
431
432 214

431 215 **2.4 Calculations**

433 216 The carbonate system is characterised through knowing any two parameters out of TA,
434
435 217 DIC, pCO_2 or pH and then using equilibrium equations and constants (Park, 1969) and the
436
437 218 CO_2SYS program (Lewis et al., 1998) to calculate the remaining parameters. The shelf wide
438
439 219 UK-SSB measurements of DIC, TA temperature, salinity and nutrient data, were used to
440
441 220 calculate pH (free scale, as recommended by Waters & Millero, 2013), pCO_2 , calcite (Ω_c) and
442
443 221 aragonite (Ω_a) saturation using the CO_2SYS program (Lewis et al., 1998) with the Mehrbach
444
445 222 constants (according to Dickson & Millero, 1987). Known uncertainties associated with
446
447 223 calculations in CO_2SYS using bottle DIC and TA results as inputs lead to an uncertainty of
448
449 224 $\pm 6 \mu\text{atm}$ in the calculation of pCO_2 (eg: Millero et al., 2002). These arise from inaccuracies in
450
451 225 the measurements and in the determination of dissociation constants. Calculated pCO_2 values
452
453 226 were checked against direct measurements of pCO_2 measured by underway systems on 60
454
455 227 occasions on-board the RV *Cefas Endeavour* and RRS *Discovery* research vessels. The average
456
457 228 difference was 2 μatm with a variation of up to $\pm 27 \mu\text{atm}$ between the calculated and measured
458
459 229 pCO_2 . We calculated pH from DIC and TA, despite this pair not being ideal for this purpose
460
461 230 (errors will be ± 0.006 ; Millero et al., 2002), in order to give a general picture of seasonal and
462
463 231 regional variations in pH on the shelf.

464
465 232 The thermal and non-thermal components of pCO_2 were calculated by assessing the
466
467 233 change in pCO_2 relative to the average of all winter data in the survey, the winter mean state
468
469 234 (386 μatm), then calculating the thermal component at the mean winter temperature (9.1°C)
470
471 235 following Takahashi et al., (2002). The residual between the total and thermal component of
472
236 change was calculated to assess the non-thermal, or largely biological, component.

473
474
475
476
477
478
479
480
481
482
483
484
485
486
487
488
489
490
491
492
493
494
495
496
497
498
499
500
501
502
503
504
505
506
507
508
509
510
511
512
513
514
515
516
517
518
519
520
521
522
523
524
525
526
527
528
529
530
531

238 3.0 Results

239 All results are presented with January to March defined as winter, April-June as spring,
240 July-September as summer and October-December as autumn when describing the seasonal
241 distribution in biogeochemical variables. Table 1 shows the seasonal mean average (and
242 standard deviation) for each variable and region. As the sampling was not distributed evenly in
243 space and time some regions remain under-sampled, especially the Minches (region 6) in
244 autumn and in the Norwegian Trench (region 9), as indicated in Table 1.

246 3.1 Hydrographic variability

247 Figure 2 shows the seasonal variation in sea surface temperature (SST) around an
248 average of 14 °C. The coldest surface waters (average 7.65 °C) were seen in winter, especially
249 in the North Sea (region 1, Table 1a). The warmest surface waters were generally observed to
250 the south and in the summer, (eg: average of 18.27 °C Eastern English Channel (region 3).
251 Warm sea surface temperatures (16.69 °C), were still apparent in the autumn in the Eastern
252 English Channel (region 3). Overall the regional variations were dominated by a decrease in
253 SST to the north (Figure 2).

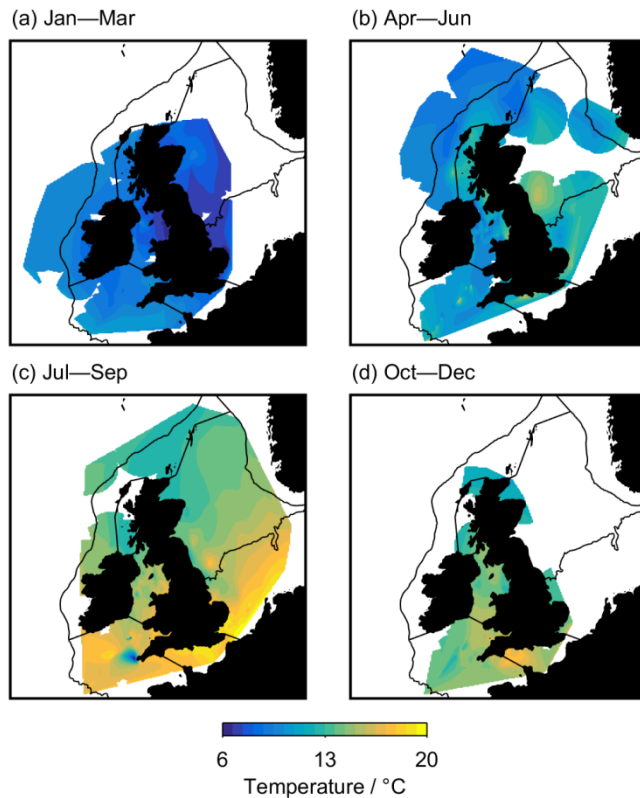
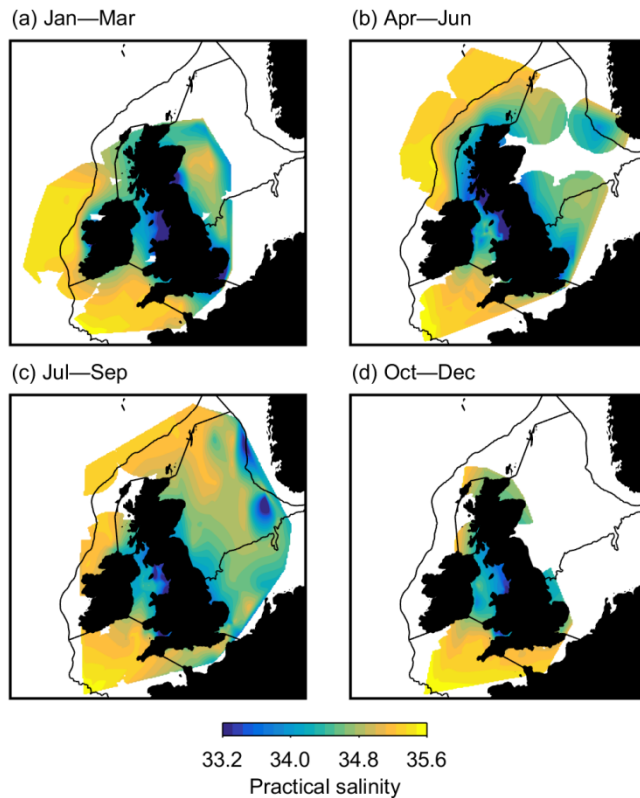


Figure 2: Seasonal maps of sea surface temperature (SST), using sensor data taken at the point of sampling on the SSB surveys. Figures 2-9, 12-15 are all mapped from 48 to 62°N, 16°W to 8°E showing winter (Jan-Mar), spring (Apr-Jun), summer (Jul-Sep) and autumn (Oct-Dec).

Figure 3 shows the seasonal and regional variation in sea surface salinity (SSS). Regional variation dominated over seasonal variability and the shelf waters were fresher than the oceanic waters. The mean SSS for the whole data set was 34.5 with higher salinities from oceanic influence observed to the west on the Atlantic northwest approaches (35.6, region 8). A tongue of high salinity water was observed in the northern North Sea (region 1). This feature was especially prominent in summer (Figure 2, where the average SSS was 34.6, Table 1a), showing the influence of the advection of Atlantic water into this region.



268

269 **Figure 3:** Seasonal maps of sea surface salinity (SSS) as practical salinity, using sensor data
 270 taken at the point of sampling on the SSB surveys.

271

272 3.2 Chemical variability

273 3.2.1 Nutrients

274 Figures 4 and 5 show the seasonal and regional variation in surface inorganic nutrients.
 275 Generally nitrate concentrations were relatively high offshore, in the Atlantic waters off shelf
 276 (region 7) compared to the inner shelf regions in all seasons. In contrast, the silicate
 277 concentrations were generally lower on the outer shelf compared with the inner shelf (see
 278 Figure 4 and 5). For example to the west of Ireland (in region 7) the average nitrate
 279 concentration in winter was relatively high ($7.9 \mu\text{mol kg}^{-1}$) when the silicate concentrations
 280 were relatively low ($4.6 \mu\text{mol kg}^{-1}$) as shown in Table 1.

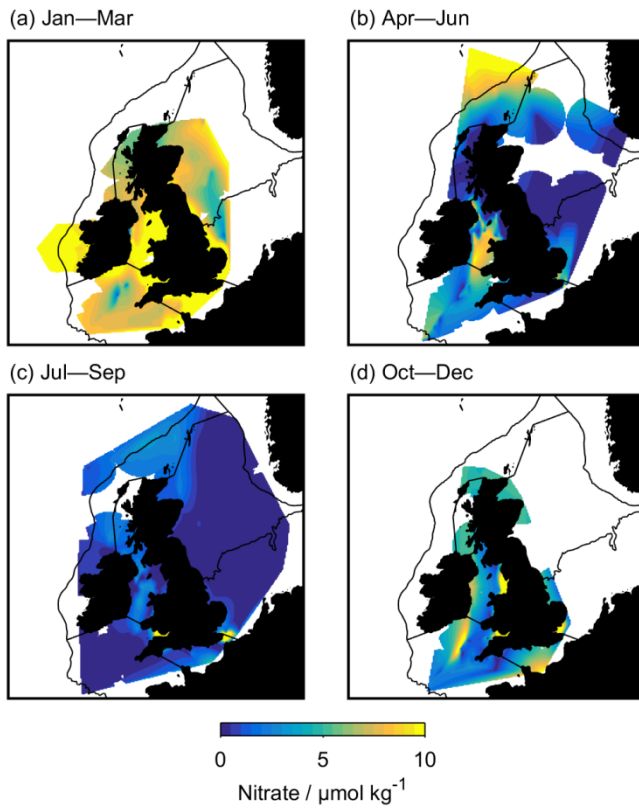
281 Seasonally the highest nitrate and silicate concentrations were observed in winter, in all
 282 regions (Figures 4 and 5). For example, the winter nutrient concentrations were high in the
 283 Irish Sea (region 5) with average winter nitrate and silicate of $9.9 \mu\text{mol kg}^{-1}$ and $7.5 \mu\text{mol kg}^{-1}$

650
651
652 284 ⁻¹ respectively. However, relatively low nitrate concentrations (6.3 $\mu\text{mol kg}^{-1}$) were observed
653
654 285 in winter off the Scottish west coast (region 6).

655 286 In spring the lowest nitrate concentrations were observed in the northern North Sea
656
657 287 (average 0.5 $\mu\text{mol kg}^{-1}$, region 1) and the Minches (1.0 $\mu\text{mol kg}^{-1}$, region 6) but remained
658
659 288 relatively high offshore to the north of Scotland (6.7 $\mu\text{mol kg}^{-1}$, region 8) and in the Irish Sea
660
661 289 (3.9 $\mu\text{mol kg}^{-1}$, region 5). By summer, nitrate concentrations were depleted in most regions
662
663 290 (Figures 4 and 5). However in Liverpool Bay (in region 5), nutrient concentrations were never
664
665 291 fully depleted although the largest seasonal changes were observed here, with a winter to
666
667 292 summer decrease of 8 $\mu\text{mol kg}^{-1}$ for nitrate and 5 $\mu\text{mol kg}^{-1}$ for silicate (see also Tables 1a and
668
669 293 1b). On the Scottish continental shelf (region 7), to the northeast of Scotland, nitrate
670
671 294 concentrations also remained above detection (average 1.2 $\mu\text{mol kg}^{-1}$) into summer. In the
672
673 295 autumn, nutrient concentrations had started in increase in Liverpool Bay (in region 5), earlier
674
675 296 than in other regions (Figures 4 and 5).

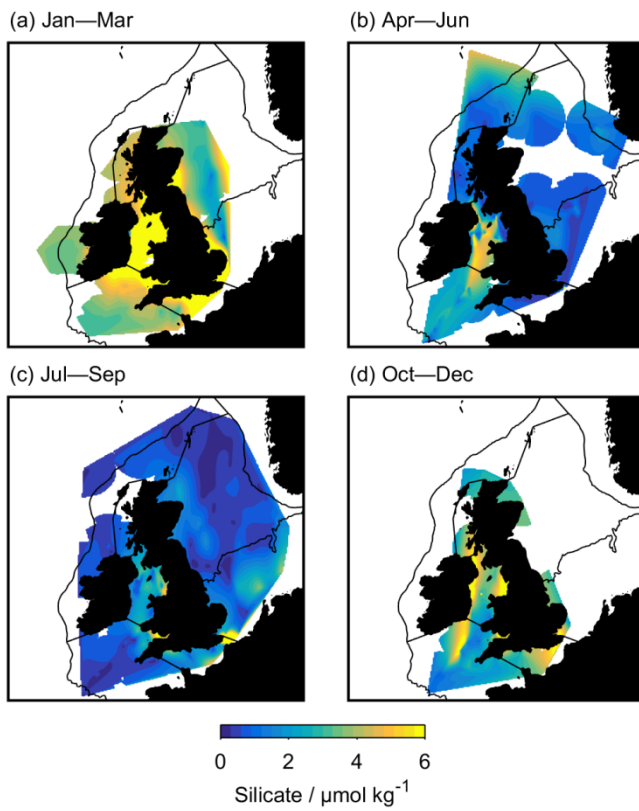
676 297 Phosphate concentrations were measured but have not been mapped here as they were
677
678 298 uniform around the whole of the UK shelf (with a winter mean of 0.55 $\mu\text{mol kg}^{-1}$, Table 1a),
679
680 299 although some deviations in the ratio of nitrate to phosphate are discussed in section 4.1.

681 300
682
683
684
685
686
687
688
689
690
691
692
693
694
695
696
697
698
699
700
701
702
703
704
705
706
707
708



302

303 **Figure 4:** Seasonal maps of sea surface nitrate concentrations, from SSB bottle samples.



304

305 **Figure 5:** Seasonal maps of silicate concentrations, from SSB bottle samples.

768
769
770
771
772
773
774
775
776
777
778
779
780
781
782
783
784
785
786
787
788
789
790
791
792
793
794
795
796
797
798
799
800
801
802
803
804
805
806
807
808
809
810
811
812
813
814
815
816
817
818
819
820
821
822
823
824
825
826

3.2.2 Total Alkalinity

Figure 6 shows the seasonal and regional TA distribution. The annual mean TA for the whole dataset was $2320 \mu\text{mol kg}^{-1}$. There was a relatively large range of values, especially in the northern North Sea (region 1), where the seasonal mean TA increased from $2275 \mu\text{mol kg}^{-1}$ in spring to $2310 \mu\text{mol kg}^{-1}$ in winter (Table 1b). In the high salinity Atlantic waters of the northwest approaches (region 8), seasonal mean TA values were relatively high (above $2330 \mu\text{mol kg}^{-1}$) and the seasonal range was small (Table 1b). Overall, TA distribution was generally similar to salinity with higher TA offshore throughout the year and the lowest values on the shelf.

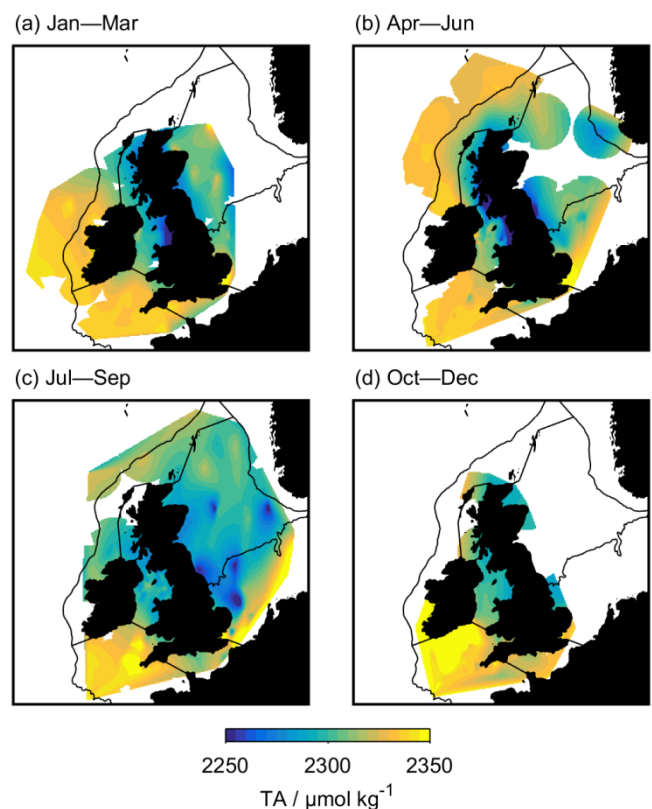


Figure 6: Seasonal maps of total alkalinity (TA) measurements, from SSB bottle samples.

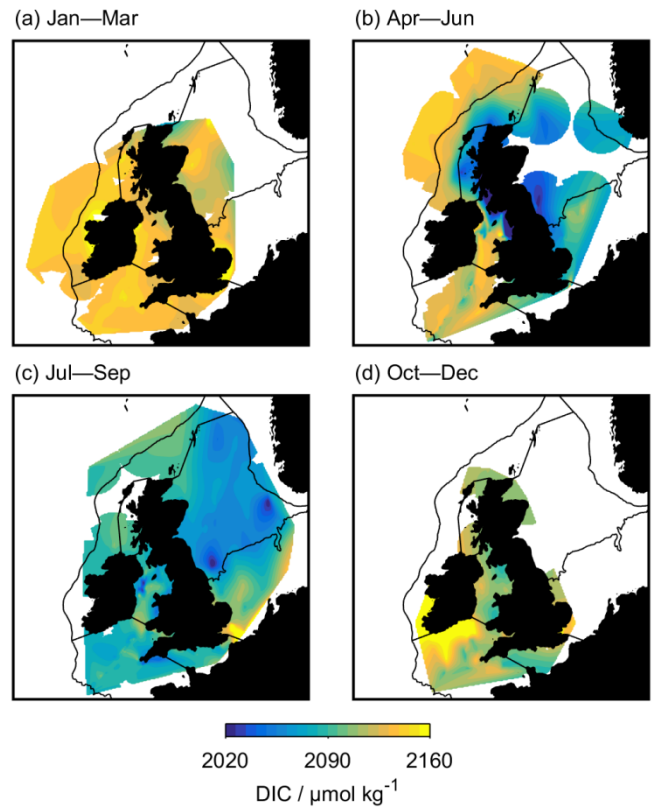
3.2.3 Dissolved Inorganic Carbon

Figure 7 shows the seasonal and regional distribution of DIC. The largest seasonal change in DIC was in the northern North Sea (region 1) where there was over $100 \mu\text{mol kg}^{-1}$

827
828
829
830
831
832
833
834
835
836
837
838
839
840
841
842
843
844
845
846
847
848
849
850
851
852
853
854
855
856
857
858
859
860
861
862
863
864
865
866
867
868
869
870
871
872
873
874
875
876
877
878
879
880
881
882
883
884
885

322 decrease in the seasonal mean DIC from winter to spring (Figure 7, Table 1b). The lowest DIC
323 concentrations observed were in spring in the northern North Sea ($2034 \mu\text{mol kg}^{-1}$, region 1)
324 and the Minches (region 6, around $2065 \mu\text{mol kg}^{-1}$) and in summer on the continental shelf
325 (region 7, around $2097 \mu\text{mol kg}^{-1}$, Table 1b). DIC concentrations peaked in winter and
326 decreased in the spring and summer in all regions (Table 1b), therefore DIC showed a similar
327 distribution to nutrient concentrations.

328



329

330 **Figure 7:** Dissolved Inorganic Carbon (DIC) measurements, from SSB bottle samples.

331

332 3.2.4 Partial pressure of carbon dioxide

333 Figure 8 shows the seasonal and regional variations in measured and calculated $p\text{CO}_2$.
334 Taking an atmospheric $p\text{CO}_2$ of $400 \mu\text{atm}$ (Humphreys et al., this issue) then under-saturated
335 values (relative to atmospheric $p\text{CO}_2$) are indicated by the blue colours and over-saturated by
336 the warmer colours in Figure 8. Generally, the highest values were seen in the autumn and the
337 lowest values for each region were in the spring (Figure 8).

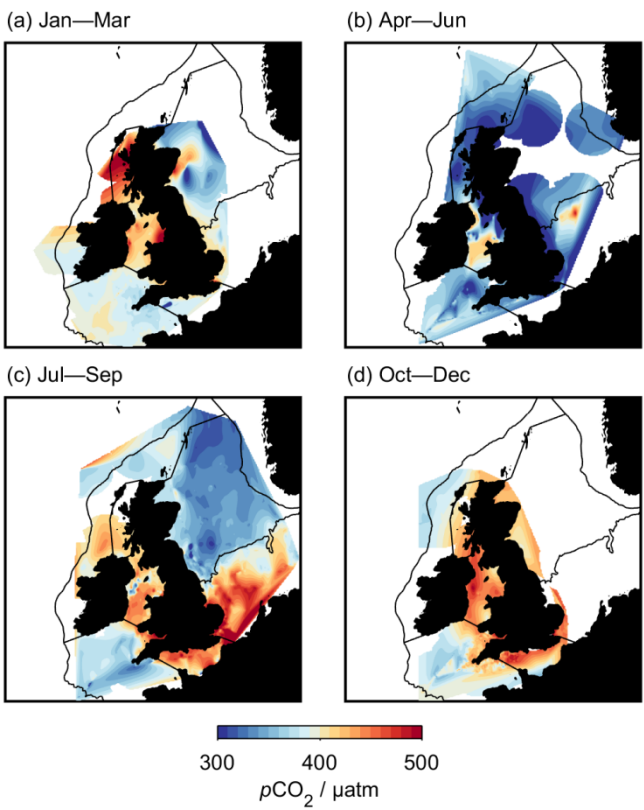
338 In the seasonally stratified northern North Sea (region 1) $p\text{CO}_2$ values were generally
339 under-saturated from winter ($352 \mu\text{atm}$, Table 1b) to summer. However, there is some variation

886
887
888
889
890
891
892
893
894
895
896
897
898
899
900
901
902
903
904
905
906
907
908
909
910
911
912
913
914
915
916
917
918
919
920
921
922
923
924
925
926
927
928
929
930
931
932
933
934
935
936
937
938
939
940
941
942
943
944

340 within this region where relatively oversaturated values were observed close to the Scottish
341 coast from autumn to winter (Figure 8). The largest seasonal variation in $p\text{CO}_2$ was observed
342 in the southern North Sea, (region 2) with an increase of over $100 \mu\text{atm}$ between the spring and
343 autumn (Figure 8, Table 1b).

344 A seasonal over-saturation in CO_2 was especially prominent in the relatively shallow
345 inner shelf regions in summer and autumn (Figure 8 and Table 1b). For example, a marked
346 increase in $p\text{CO}_2$ from spring to summer was observed in the relatively shallow eastern English
347 Channel (region 3, from 333 to $452 \mu\text{atm}$, Table 1b).

348



349

350 **Figure 8:** Surface $p\text{CO}_2$, calculated from bottle samples analysed for DIC/TA (using
351 CO_2SYS) and measured $p\text{CO}_2$ from underway systems on the RRS *Discovery* and RV *Cefas*
352 *Endeavour* (2014-2015).

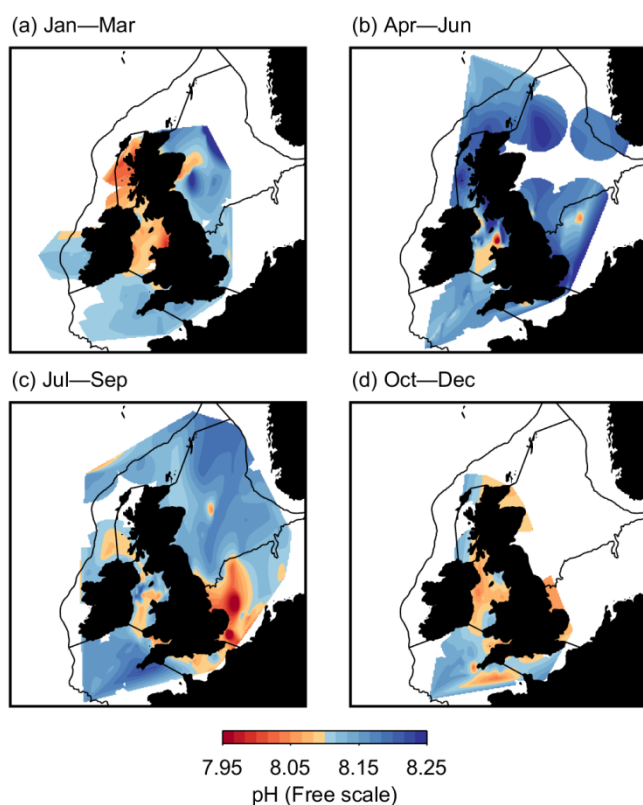
353

354 In the Celtic Sea (region 4) $p\text{CO}_2$ was predominantly under-saturated throughout the
355 year (Figure 8). However, $p\text{CO}_2$ increased near to the coast in autumn when the average was
356 $407 \mu\text{atm}$ (Table 1b). In contrast, the relatively shallow Irish Sea (region 5) showed a general

357 year round over-saturation in $p\text{CO}_2$ (with seasonal averages above $409 \mu\text{atm}$, Table 1b) except
358 for in spring.

359 3.2.5 Calculated pH

360 Figure 9 shows the seasonal and regional variation in calculated pH around the shelf. It
361 is important to note that the colour scale is reversed in Figure 9 for easier comparisons with
362 $p\text{CO}_2$ as an inverse relationship is expected. Overall, calculated pH was lowest around the
363 coast in autumn and the highest calculated pH was observed in spring (Figure 9). For example
364 in the northern North Sea (region 1) the seasonal mean pH in spring was 8.19 when $p\text{CO}_2$ was
365 low (see Table 1b). In the southern North Sea (region 2) there was a spring to summer decrease
366 in the calculated pH (from 8.15 to 8.05, Table 1b). Likewise, in the eastern Channel (region 3)
367 the pH decreased to a similar extent from spring to summer (Table 1b). In the Irish Sea (region
368 5) and the Minches (region 6) the seasonal mean pH was lowest in winter (when $p\text{CO}_2$ was
369 high) and increased in the spring (from 8.06 to 8.18 in region 6, Table 1b).



371
372 **Figure 9:** pH (freescale), calculated from bottle samples analysed for DIC/TA (using
373 CO_2SYS).

1004
1005
1006
1007
1008
1009
1010
1011
1012
1013
1014
1015
1016
1017
1018
1019
1020
1021
1022
1023
1024
1025
1026
1027
1028
1029
1030
1031
1032
1033
1034
1035
1036
1037
1038
1039
1040
1041
1042
1043
1044
1045
1046
1047
1048
1049
1050
1051
1052
1053
1054
1055
1056
1057
1058
1059
1060
1061
1062

374

4.0 Discussion

375

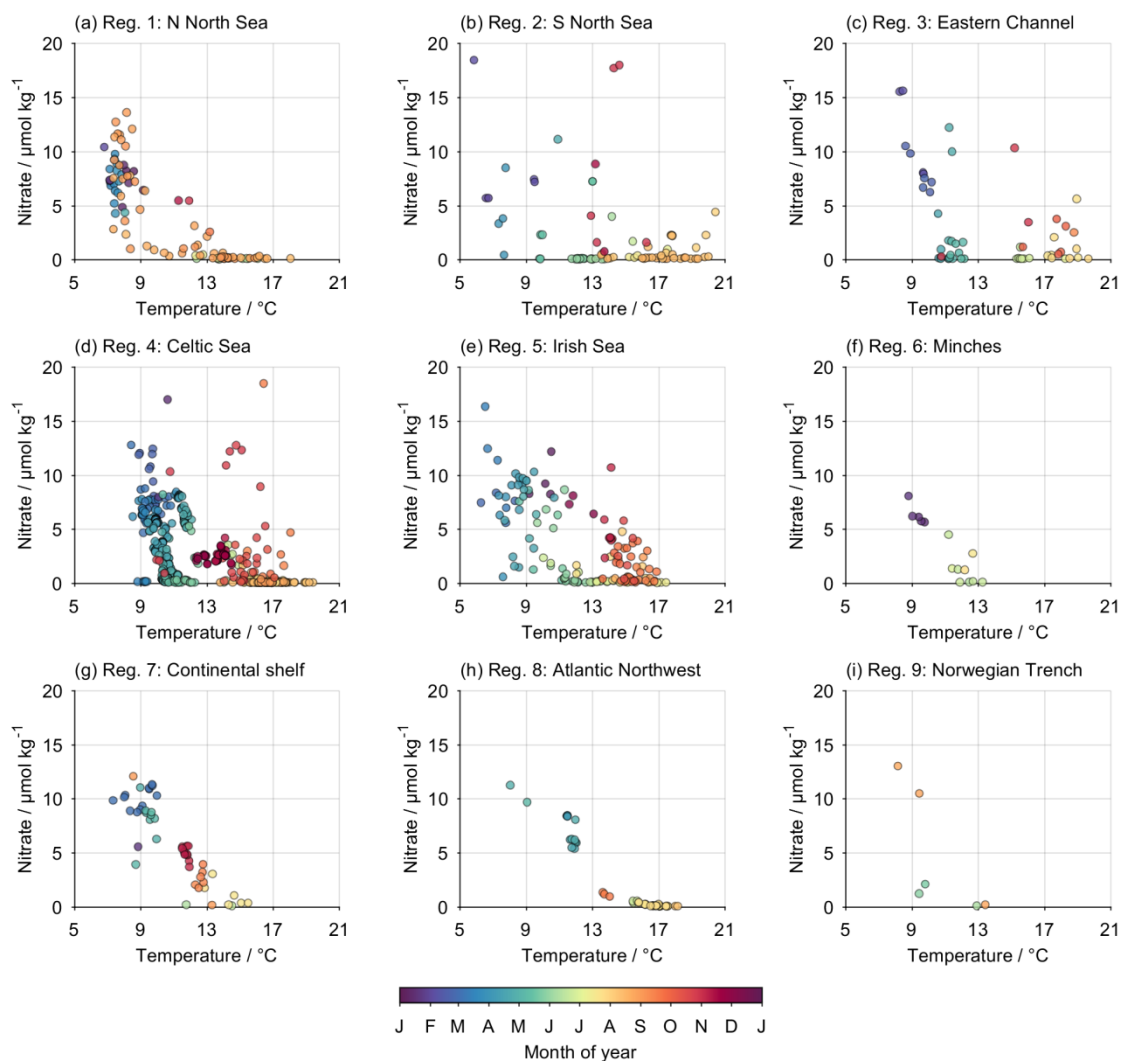
4.1 An overview of seasonal variations in relation to regions

376

Dividing the UK-SSB dataset into 9 ecohydrodynamic regions revealed large regional variations in carbonate chemistry parameters in relation to nutrients and hydrography. Figure 10 illustrates the relationship between hydrography (SST) and surface nutrient concentrations for each of the regions considered.

377

378



382

383

Figure 10: Measured nitrate concentrations and sea surface temperature for each month and region.

384

385

1063
1064
1065 386 Overall, there was a winter peak in nutrient concentrations, then a rapid decrease in the
1066 387 spring and summer months. The rapid depletion in nitrate (and DIC) concentrations in spring
1067 388 are likely to result from their assimilation in the production of organic material by
1068 389 phytoplankton, during the ‘spring bloom’ (Frigstad et al., 2015). The dominant pattern on the
1069 390 shelf was for low nitrate concentrations throughout the spring to summer months, in warming
1070 391 water. Then, in the autumn months there was an increase in nitrate concentrations (as the water
1071 392 cools), observed in all regions where data were available (Figure 10). The increase in nitrate
1072 393 concentrations during autumn months is likely to be due to the remineralisation of organic
1073 394 matter, the break down the thermal stratification of the surface waters and the onset of vertical
1074 395 mixing. This seasonal variability is as expected at temperate latitudes (Smith et al., 2014) and
1075 396 gives a triangular distribution to the data points (Figure 10). Similar patterns would be expected
1076 397 for DIC, especially in winter months when seasonal stratification breaks down and nitrate plus
1077 398 DIC accumulates in the surface waters.

1086 399 The winter peak in nutrient (and DIC) concentrations are also likely due to organic
1087 400 matter remineralisation and the convective mixing of colder high nutrient and DIC rich waters
1088 401 from below (Körtzinger et al., 2008). Maximum concentrations were reached just before the
1089 402 return of stratification in spring in all regions (Figure 10). However, in the Northern North Sea
1090 403 the autumn SST is relatively cold and associated with higher nitrate concentrations compared
1091 404 with other regions (Figure 10). The relationship between SST and nitrate concentrations is less
1092 405 clear in the Southern North Sea (region 2, Figure 10). Relatively low salinities were observed
1093 406 in the east of the southern North Sea in summer (region 2, in Figure 3) due to fresh water
1094 407 entering the North Sea from the major European continental rivers (such as the Rhine).
1095 408 Therefore, riverine inputs are likely to have contributed to the higher nitrate concentrations
1096 409 seen in this region.

1100 410 In the well mixed eastern English Channel (region 3) there was a pronounced
1101 411 ‘triangular’ shape in the relative nitrate and SST variability (Figure 10). The nitrate
1102 412 concentrations increased earlier in the year (compared with other regions), starting in the
1103 413 summer whilst SST was still relatively high. This may be due to the continuous injection of
1104 414 nutrients into the euphotic zone that is seen in many well mixed systems (L’Helguen et al.,
1105 415 1996). High nitrate (and silicate, Figure 5) concentrations were observed for most of the year
1106 416 in the eastern Channel (region 3), probably from the remineralisation of organic material in
1107 417 these relatively shallow and well-mixed regions.

1122
1123
1124 418 In the western English Channel and the Celtic Sea (region 4), an area characterised by
1125 419 seasonal thermal stratification (Smyth et al., 2010; Smith et al., 2014), the highest nitrate
1126 420 concentrations were generally observed in the winter (Figure 10, from January to March). In
1127 421 the central Irish Sea (region 5) nitrate was never depleted, even during spring and summer,
1128 422 possibly due to riverine inputs (Greenwood et al., 2011). The seasonal mean salinity remained
1129 423 relatively low (~33.9, Table 1a) throughout the year in the Irish Sea and Liverpool Bay (region
1130 424 5) showing a high influence of fresh water input to the region (Hydes & Hartman, 2012;
1131 425 Greenwood et al., 2011). Silicate concentrations in the Irish Sea (region 5) were at least 1 μmol
1132 426 kg^{-1} higher than other regions throughout the year (Figure 5), probably due to this riverine
1133 427 influence. Seasonal coverage is relatively poor for the Minches (region 6) and the Norwegian
1134 428 trench (region 9), as seen in Figure 10.

1142 429 In the more open ocean continental shelf (region 7) and Atlantic northwest approaches
1143 430 (region 8) there was a linear relationship between nitrate and temperature, likely due to the
1144 431 spring nitrate depletion and autumn nitrate regeneration (Figure 10). To the far north of
1145 432 Scotland (in region 7) nitrate concentrations remained high ($> 5 \mu\text{mol kg}^{-1}$) until the summer
1146 433 months (Figure 10), probably due to the general northward delay in bloom timing (Siegel et
1147 434 al., 2002). From the linear relationship seen in Figure 10 the nitrate concentrations could
1148 435 almost be predicted from SST, as shown by Sathyendranath et al., (2001); Henson et al., (2003).

1153 436 1154 437 **4.2 Stoichiometry**

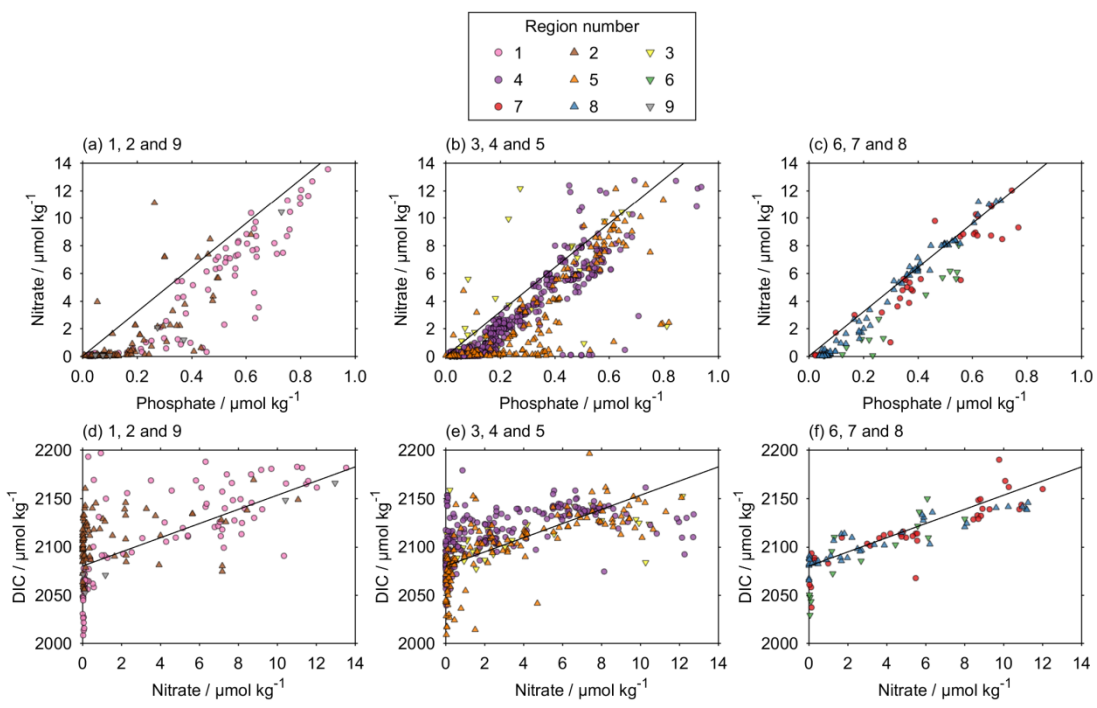
1155 438 Figures 11(a-c) shows the relationship between nitrate and phosphate. These figures
1156 439 confirm the similarity in spatial distributions between nitrate and phosphate, although most of
1157 440 the values were below the open ocean ‘Redfield’ stoichiometric ratio of 16:1 (Redfield et al.,
1158 441 1963; Anderson and Sarmiento, 1994). In the present study, some especially low nitrate values,
1159 442 relative to phosphate concentrations, were seen in both the southern North Sea (region 2, Figure
1160 443 11a) and the Irish Sea (region 5, Figure 11b). Likewise there is a relatively low N:P in the
1161 444 Celtic Sea (region 4, Figure 11b). The N:P relationship approaches the 16:1 (Anderson and
1162 445 Sarmiento, 1994) ratio in the more Atlantic influenced off shelf areas (regions 6-8, Figure 11c).

1163 446 Nutrient concentrations are likely to be higher near the coast than in the open ocean,
1164 447 particularly where there are riverine inputs. However, a key feature established in the North
1165 448 Sea Project data (Hydes et al., 1999) was that the maximum nitrate concentrations observed in
1166 449 the Central North Sea (Hydes et al., 1999) and in the Irish Sea (Gowen et al., 2002 and 2008)

1181
 1182
 1183
 1184
 1185
 1186
 1187
 1188
 1189
 1190
 1191
 1192
 1193
 1194
 1195
 1196
 1197
 1198
 1199
 1200
 1201
 1202
 1203
 1204
 1205
 1206
 1207
 1208
 1209
 1210
 1211
 1212
 1213
 1214
 1215
 1216
 1217
 1218
 1219
 1220
 1221
 1222
 1223
 1224
 1225
 1226
 1227
 1228
 1229
 1230
 1231
 1232
 1233
 1234
 1235
 1236
 1237
 1238
 1239

450 were below those observed in ocean waters adjacent to the shelf (Hydes et al., 2004). This
 451 resulted in low nitrate to phosphate (N:P) ratios (Hydes et al 1999; Gowen et al., 2002),
 452 probably from denitrification in the sediments of these relatively shallow (and well mixed) seas
 453 (Setzinger and Giblin., 1996). Recently Kitidis et al. (2017) also showed that sediment
 454 anaerobic ammonium oxidation and denitrification removed 6-9 % of the nitrate in the Celtic
 455 Sea over an annual cycle.

456 Figures 11(d-f) show the relationship between DIC and nitrate. Overall, there was a
 457 positive correlation between DIC and nitrate around the northwest European Shelf. However
 458 there was large variability in this relationship within and between the regions. For example in
 459 the northern North Sea (region 1) most points were above the line shown in Figure 11d (that
 460 represents the open ocean C:N of 7.3, Anderson and Sarmiento, 1994). In the southern North
 461 Sea (region 2) there was a pronounced variability in the C:N relationship at very low nitrate
 462 concentrations (Figure 11d). In the Celtic Sea (region 4) there was a variation in the C:N ratio
 463 as the nutrient concentration increased (Figure 11e). However, on the Irish and Scottish shelf
 464 (region 7) most of the points followed this line (Figure 11f).



466
 467
 468 **Figure 11:** A comparison of the (a-c) nitrate and phosphate concentrations (in groups of 3
 469 regions for ease of viewing) showing the Anderson and Sarmiento (1994) N:P ratio of 16:1 as

1240
1241
1242 470 a solid line and (d-f) the relationship between DIC and nitrate with the C:N ratio of 7.3 as a
1243 solid line (Anderson and Sarmiento, 1994).
1244 471
1245
1246 472

1247 473 A positive correlation was generally observed between DIC and nitrate, as both are
1248 influenced by productivity and the breakdown of organic material. Where the variability in the
1249 474 C:N relationship was pronounced at very low nitrate concentrations, for example in the
1250 475 southern North Sea (region 2), this may be a further indication of denitrification. This process
1251 is significant in the North Sea (Hydes et al, 1999) and could contribute to the relatively low
1252 476 nitrate values observed in both the N:P and C:N ratios (Figure 11) in this region. However,
1253 477 riverine input can be an additional source of variability in the C:N relationship in the more
1254 coastal systems through both nutrient input (Greenwood et al., 2011) and DIC input (McGrath
1255 478 et al., 2016).
1256
1257 479

1258 480
1259
1260 481
1261 482 In the Celtic sea (region 4), the points were above the line at low nitrate concentrations
1262 and below the line at higher concentrations ($> 8 \mu\text{mol kg}^{-1}$, Figure 11e). So, the C:N ratio was
1263 483 initially high in the potentially productive periods (periods of productivity were identified for
1264 484 the Celtic Sea by Hickman et al., this issue), when nitrate concentrations were lower. Then the
1265 C:N decreased at high nitrate concentrations. High C:N suggests a more efficient recycling of
1266 485 nitrate compared with carbon and that the organic material exported from the surface would be
1267 carbon enriched (Sambrotto et al., 1993). Therefore spatial and seasonal changes in C:N could
1268 486 have a significant impact on carbon cycling and export off the shelf via the continental shelf
1269 487 pump (Gruber and Galloway, 2008; Painter et al., 2017). Variation in the C:N will also have
1270 implications for methods that calculate productivity from the depletion in DIC or nitrate
1271 488 (Frigstad et al., 2015 and references therein) using the 'standard' C:N Redfield ratio of 6.6:1
1272 (Anderson and Sarmiento, 1994).
1273 489
1274 490
1275
1276 491
1277
1278 492
1279 493
1280
1281 494

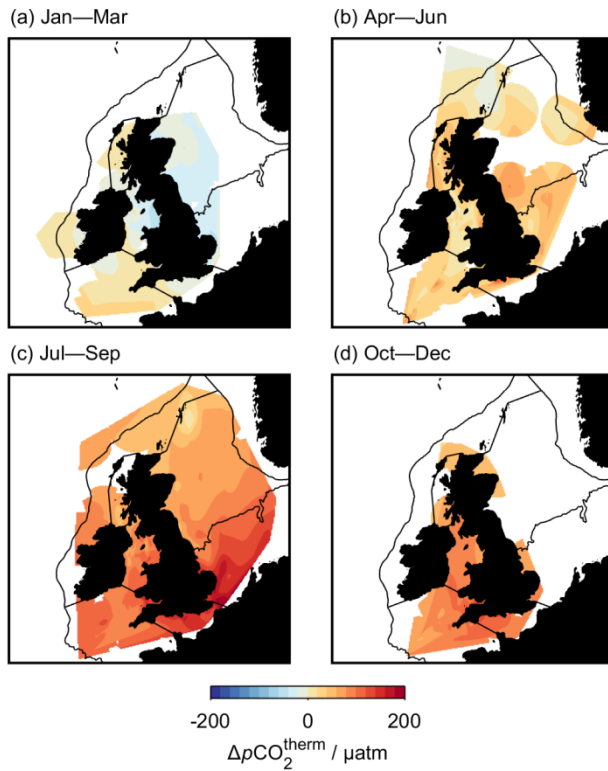
1282 495 **4.3 Controls on seawater pCO₂**

1283
1284 496 The solubility of CO₂ depends mainly on temperature (increased solubility at low
1285 497 temperature, decreased at high temperatures). In turn, biological production processes tend to
1286 498 decrease surface water pCO₂, whereas respiration and remineralisation processes tend to
1287 increase surface water pCO₂ (Shadwick et al., 2011). The dominance of these processes varies
1288 499 through the year and with region (Takahashi et al., 2002; Jiang et al., 2013). To study this
1289 500 further we assessed the physical and biological forcing on pCO₂. Figure 12 shows the thermal
1290
1291 501
1292
1293
1294

1299
1300
1301 502 component of the change in pCO₂ calculated following Takahashi et al. (2002). Figure 13
1302
1303 503 shows the residual between the total and thermal component of change and represents the non-
1304
1305 504 thermal component, which we assume to be largely biologically driven. This is either through
1306 505 the remineralisation of organic matter in the surface layer, or the addition of remineralised
1307
1308 506 nutrients from the deep layer through vertical mixing. The magnitude of this component may
1309
1310 507 be reduced by any air-sea gas exchange.

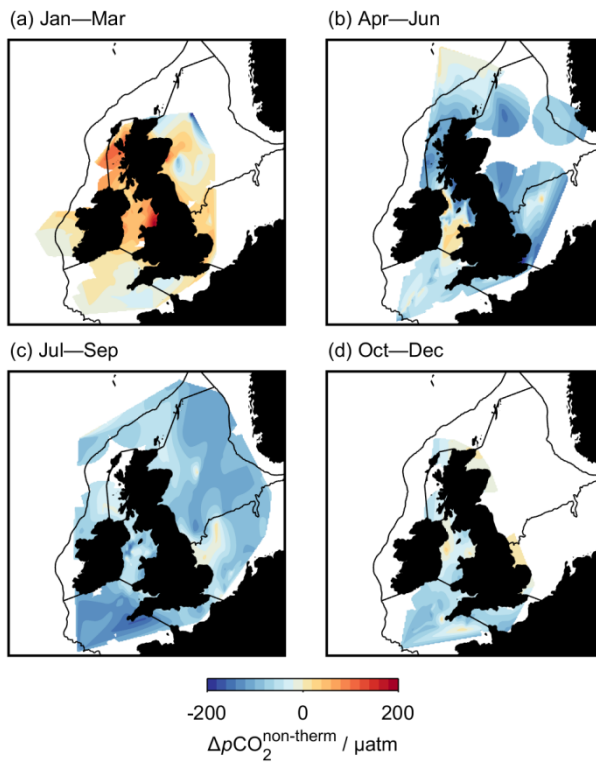
1311 508 Our study showed the dominance of thermal control (Figure 12) on the pCO₂ especially
1312
1313 509 in the spring and summer. Temperature can be the main factor influencing the pCO₂ variability,
1314
1315 510 through the control on stratification and stabilisation of the water column triggering production.
1316 511 The spring time decrease in pCO₂, to under saturated levels was seen in all regions and
1317
1318 512 coincided with a large decrease in nutrients in these productive waters (Table 1), as shown by
1319 513 Thomas et al., (2005). Biological production can impact surface pCO₂ in summer in stratified
1320
1321 514 systems by the presence of subsurface phytoplankton blooms below the (shallow) thermocline
1322 515 (Shadwick et al., 2011). Non-thermal or biological control dominated from autumn through to
1323
1324 516 winter (Figure 13) due largely to regeneration from the respiration of organic material.

1325 517 There were clear regional variations in the balance of thermal and non-thermal controls.
1326
1327 518 For example in the central region of the northern North Sea (region 1) there was a thermally
1328
1329 519 driven increase in pCO₂ of about 70 µatm from winter to spring (Figure 12), and a non-thermal
1330 520 decrease of 110 µatm (Figure 13). This region seasonally stratifies and DIC is transported off
1331
1332 521 shelf (Huthnance et al., 2009). Overall, in the seasonally stratified northern North Sea (region
1333 522 1), the control of pCO₂ was predominantly non-thermal (biological, as shown in Figure 13), as
1334
1335 523 has been shown previously (Thomas et al, 2005 & 2006; Van Leeuwen et al., 2015). In contrast,
1336
1337 524 in the well-mixed, shallower southern North Sea (region 2) thermal controls on pCO₂
1338 525 dominated (Figure 12). In this region, water temperature was the dominant control on both
1339
1340 526 pCO₂ and nutrient concentrations (Thomas et al, 2005 & 2006; Van Leeuwen et al., 2015).



529

530 **Figure 12:** The thermal component of the change in pCO₂ calculated following Takahashi et
 531 al. (2002).



532

533 **Figure 13:** The non-thermal component of the change in pCO₂ (calculated following Takahashi
 534 et al., 2002 as the residual between the total and thermal component of change).

1417
1418
1419 535
1420
1421 536 Our study suggested that the eastern English Channel (region 3) was over-saturated in
1422 CO₂ in the autumn (Figure 8). This was when non-thermal heterotrophic processes, such as
1423 537 organic matter remineralisation, dominated (Figure 13). An autumnal over-saturation of CO₂
1424 538 has been observed previously in the eastern English Channel (Frankignoulle et al., 1996; Jiang
1425 539 et al., 2013). Borges (2005) also suggested that the permanently well-mixed and shallow
1426 540 ecosystems within the eastern English Channel were seasonally over-saturated and a seasonal
1427 541 source of CO₂.
1428 542

1432 543 Overall pCO₂ in the Celtic Sea (region 4) was close to the atmospheric pCO₂ for most
1433 of the year (Figure 8), with a pronounced under-saturation in spring (to a mean average of 364
1434 544 µatm, Table 1). This is similar to the observations made by Kitidis et al., (2012). The seasonal
1435 545 variations in pCO₂ were dominated by biology rather than advection in the northern part of the
1436 546 western English Channel (Figure 13). In contrast, the data suggested that in the Irish Sea
1437 547 (region 5) pCO₂ was over-saturated for most of the year (Figure 8). There was a dominance of
1438 548 non-thermal controls on pCO₂ in autumn and winter in the Irish Sea (region 5), and the non-
1439 549 thermal influences were especially high near to the coast (Figure 13). pCO₂ remained higher
1440 550 here than if it were in equilibrium with the atmosphere for most of the year (Table 1), except
1441 551 for in the spring when there was a pronounced under-saturation in the surface waters.
1442 552

1448 553 In the Minches (region 6), the non-thermal component was especially high in winter
1449 554 and had little influence for the rest of the year. In the wider sub-polar Atlantic, the seasonal
1450 555 cycle of pCO₂ was dominated by the mixing of cold water (leading to increased CO₂ solubility).
1451 556 This was seen to the west of Ireland (region 7) where both the thermal and non-thermal
1452 557 components increased pCO₂ in the autumn and winter.

1456 558 In summary, the largest thermal component observed was in the summer to the south
1457 559 of the UK (Figure 12), especially in the southern North Sea (region 2) and the eastern English
1458 560 Channel (region 3) where the highest SST had been observed in summer (Figure 2). The largest
1459 561 non-thermal component observed (Figure 13) was in winter, especially around the coast in
1460 562 Liverpool Bay (region 5) and the Minches (region 6). In all of these well-mixed and shallower
1461 563 regions, it is likely that the decaying bloom, and breakdown of organic material (Carr et al.,
1462 564 this issue), increased the pCO₂ in autumn and winter. As these regions remain mixed the pCO₂
1463 565 super-saturation persists until the next spring.

1469 566 Our seawater pCO₂ data has been used to assess potential sources and sinks around the
1470 567 shelf (Kitidis et al., 2018 in prep.). The direction of air-sea gas fluxes are driven by

1476
1477
1478 568 concentration differences between the seawater and atmosphere. Where $p\text{CO}_2$ in seawater was
1479
1480 569 under-saturated compared with the atmospheric $p\text{CO}_2$ it suggests that this area will be a sink;
1481
1482 570 if it exceeded $p\text{CO}_2$ in air then this suggests the region will be a source to the atmosphere.
1483
1484 571 However, the magnitude of the flux is modulated by other processes, for which wind speed can
1485
1486 572 be used as a proxy (Wanninkhof, 2014). This is explored further in Kitidis et al. (2018, in prep.)
1487
1488 573 and the NW European shelf was found to be net autotrophic and a CO_2 sink over the period of
1489
1490 574 our study.

1491 575 The separation into ecohydrodynamic regions (after Bresnan et al., 2015) was done to
1492
1493 576 distinguish the different hydrographical regions. These separations correspond well to the
1494
1495 577 biogeochemical variability observed from the data. However, if you go further into the details
1496
1497 578 then more complex and dynamic hydrographical systems are observed, such as tidal fronts
1498
1499 579 between the year round well-mixed and seasonally stratified ecosystems, shelf break systems
1500
1501 580 and estuarine systems. The on-shelf tidal frontal zones between the permanently well-mixed
1502
1503 581 and seasonally stratified areas are particularly productive and can influence CO_2 exchange and
1504
1505 582 examples of these frontal regions are seen in the Irish Sea (Simpson & Hunter; 1974) and in
1506
1507 583 the Celtic Sea (Pingree & Griffiths, 1978). For example within the seasonally stratified Celtic
1508
1509 584 Sea (region 4) the southern part of the western English Channel and the waters around Land's
1510
1511 585 End (Marrec et al., 2013), can be distinguished in the hydrography. Within the western Channel
1512
1513 586 and Celtic Sea (region 4) there was a clear division between the northern sub-region, where
1514
1515 587 there was a dominance of non-thermal control of $p\text{CO}_2$ in winter and the southern part where
1516
1517 588 thermal effects dominated (Figure 12).

1518 589 1519 1520 590 **4.4 Changes in alkalinity and pH**

1521 591 The TA and salinity distribution is generally similar as both are strongly influenced by
1522
1523 592 evaporation, riverine freshwater inputs and precipitation. TA can be considered as conservative
1524
1525 593 in the open ocean where TA and salinity tend to be linearly related (Lee et al., 2006; Jiang et
1526
1527 594 al., 2014). Near coastal waters, with a strong salinity gradient, are ideal places to get a TA: S
1528
1529 595 linear relationship. However in the current study the real near coastal water area was not
1530
1531 596 assessed, and it was difficult to get see a linear TA:S relationship in such diverse ecosystems
1532
1533 597 although the low salinity water was generally associated with low TA values. The offshore
1534
1535 598 increase in salinity (Figure 3) and TA (Figure 6) dominated over any seasonal variations.

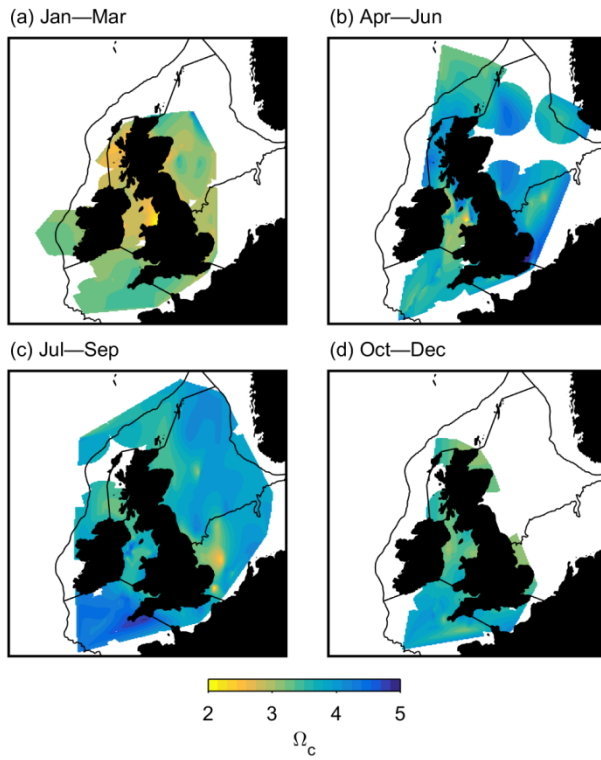
1535
1536
1537 599 Many processes result in a TA increase in near coastal waters (Cai et al., 2011; Thomas
1538 et al., 2007), such as the increase in TA by the oxidation of organic material in marine
1539 600 sediments (Froelich et al., 1979). The southern North Sea (region 2) and the eastern Channel
1540 601 (region 3) both showed large variability in TA compared with other regions as these shallow
1541 602 areas are influenced by high organic material (Salt et al., 2016). Coastal regions are also
1542 603 influenced by riverine input, where the presence of calcareous limestone bedrock can increase
1543 604 TA in shelf waters. For example, the high TA river Liffey near Dublin inputs to the Irish Sea
1544 605 (region 5) although in this case the effects will only be observed near to the coast due to a low
1545 606 riverine discharge (McGrath et al. 2016). Previous studies have shown some seasonality in TA
1546 607 due to productivity, for example Hydes & Hartman (2012) showed higher TA during the spring
1547 608 bloom in the Liverpool Bay sub-region of the Irish Sea (region 5). On the northwest European
1548 609 shelf large coccolithophore blooms can also strongly influence alkalinity and calcification will
1549 610 affect the TA and seawater pCO₂ (Harlay et al., 2010)
1550 611

1551 612 In the present study, large seasonal variations in pH were observed around the shelf,
1552 613 (up to 0.2 units, Table 1b). The pH range is influenced by DIC, TA and changes in temperature
1553 614 and by the balance between photosynthesis and respiration. There is generally an inverse
1554 615 relationship between pCO₂ and pH, due to the increase in H⁺ ions (i.e. decreased pH) when
1555 616 CO₂ dissolves in seawater (Zeebe and Wolf-Gladrow, 2001). pH increased in spring in all
1556 617 regions (Table 1b) when photosynthesis dominated over respiration. pH then decreased in
1557 618 summer in most regions (Table 1b): for example in the Southern North Sea (region 2) pH
1558 619 decreased from spring to summer (8.15 to 8.05, Table1), as respiration became more important
1559 620 (Provoost et al., 2010). Previous studies found similar large seasonal variations in pH (up to
1560 621 0.3) especially off the east coast of Scotland, around the Stonehaven time series site (Hydes et
1561 622 al., 2011; Ostle et al., 2016).
1562 623

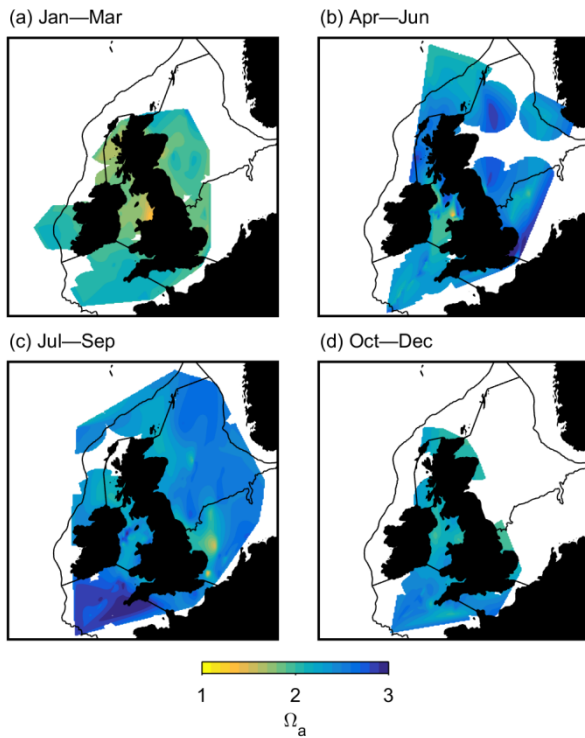
1563 624 In the North Sea (regions 1 and 2) and the eastern Channel (region 3), where
1564 625 temperature control on pCO₂ dominated, there was a winter to summer increase in pCO₂ (and
1565 626 associated pH decrease), possibly influenced by the remineralisation of organic matter in these
1566 627 shallower regions. The pCO₂ increase (and pH decrease) at the end of summer, is likely to be
1567 628 due to the influence of temperature and the remineralisation of organic matter by microbial
1568 629 processes through the sediment-water interface in these relatively shallow regions. The process
1569 630 of denitrification over muddy sediments could also influence pH although we would expect a
1570 pH increase due to this process (Froelich et al., 1979; Provoost et al., 2010).
1571
1572
1573
1574
1575
1576
1577
1578
1579
1580
1581
1582
1583
1584
1585
1586
1587
1588
1589
1590
1591
1592
1593

1594
1595
1596 631 The strong pH fluctuations in shelf seas and coastal waters (Duarte et al., 2013; Ostle
1597
1598 632 et al, 2016; Waldbusser & Salisbury, 2014) imply that the concept of ocean acidification (OA)
1599
1600 633 is difficult to transpose to coastal ecosystems, where the rates and variability of OA are higher
1601
1602 634 than in the open ocean (Doney et al., 2009). The occurrence of vibrant biological communities
1603
1604 635 in areas with large regional and seasonal variations in seawater pH imply that they possess an
1605
1606 636 inbuilt tolerance to pH changes (Bates et al., 2014; Kitidis et al., 2017). This tolerance may
1607
1608 637 occur due to the ability of seawater to buffer some of these pH changes through its alkalinity.
1609
1610 638 TA will buffer the hydrogen ions so the buffering capacity of seawater is a direct function of
1611
1612 639 TA as regions with high TA will be less prone to rapid changes in OA. The DIC:TA relationship
1613
1614 640 for example can be strongly linked to different buffer factors (eg: Egleston et al., 2010). Studies
1615
1616 641 such as ours give some indication of the present pH variability over the NW European Shelf,
1617
1618 642 which will be useful in the future in the context of ocean acidification. This study also identified
1619
1620 643 regions where the lowest TA values coincided with the lowest pH, such as the Southern North
1621
1622 644 Sea (region 2, see Table 1). The low TA may suggest regions with a decreased capacity to
1623
1624 645 buffer pH changes in the future.

1620 646 Future OA could have detrimental effects on calcifying organisms (Feely et al., 2009;
1621
1622 647 Riebesell & Tortell, 2011; Doney et al., 2011). In the current study, calcite (Figure 14) and
1623
1624 648 aragonite (Figure 15) were not generally under-saturated. Calcite saturation was always in the
1625
1626 649 range of 1.5 to 4.8 and aragonite was virtually never under-saturated (1.0 to 3.1; about 0.3% of
1627
1628 650 total measurements were <1). Aragonite is the most soluble form of calcium carbonate in the
1629
1630 651 marine environment and saturation will decrease as pH decreases (Feely et al., 2009), giving
1631
1632 652 an indication of susceptibility of a region to ocean acidification. Low saturation coupled with
1633
1634 653 low pH would affect the ability of organisms to form shells and skeletons (Fabry et al., 2008).
1635
1636 654 Model data from Artioli et al., (2014) showed localised potential under-saturation of aragonite
1637
1638 655 in the German Bight by the end of the 21st century. Changes in temperature, pCO₂ and
1639
1640 656 calcification would all further increase the vulnerability of these regions to OA in the future
1641
1642 657 (Bates et al., 2014).



660
661 **Figure 14:** Calcite saturation (Ω_c) calculated from SSB bottle DIC and TA.



663
664 **Figure 15:** Aragonite saturation (Ω_a) calculated from SSB bottle DIC and TA.

1712
1713
1714 666 As the seasonal variation in pH can be large (Ostle et al., 2016) long-term time series
1715
1716 667 measurements are required to detect any inter-annual trends (Bates et al., 2014). Ideally, over
1717
1718 668 25 years of consistently measured data are required to detect pH trends (Henson et al., 2016)
1719 669 although ICES studies in the central North Sea (Beare et al., 2013) and southern North Sea
1720
1721 670 (Duarte et al., 2013) have reported a decadal decline in pH. This decline in pH was associated
1722 671 with physical drivers (Salt et al., 2013) and changes in nutrients and eutrophication (Provoost
1723
1724 672 et al., 2010). Hydes et al., (2011) showed a trend of decreasing pH around the NW European
1725
1726 673 Shelf of -0.002 to -0.004 pH units per year between 1995 and 2009. If sample collection were
1727 674 to be continued around the shelf, the present study could be used to extend this emerging time
1728
1729 675 series.

1730 1731 676 **5.0 Conclusions**

1732
1733 677 We have synthesised the spatial distributions of nutrients and carbonate chemistry
1734 678 around the northwest European shelf. The data were divided into 9 ecohydrodynamic regions
1735
1736 679 including well-mixed inner shelf and seasonally stratified outer shelf regions. The general
1737
1738 680 trends in carbon chemistry were related to changes in the hydrography and nutrients
1739 681 (representing biological activity and riverine input). The seasonally stratified regions, (for
1740
1741 682 example off shore on the Continental slope, region 7), showed a clear inverse relationship
1742 683 between SST and surface nitrate (and DIC) concentrations. This was in contrast to the well
1743
1744 684 mixed regions, such as the eastern channel (region 3), where the regeneration of nutrients
1745
1746 685 occurred at higher temperatures. The regional variations in the DIC to nutrient relationship will
1747 686 have implications for calculations of carbon export.

1748
1749 687 The effects of thermal and non-thermal processes influencing pCO₂ have been shown
1750 688 for different seasons and regions. For example in the near-shore and relatively shallow
1751
1752 689 ecosystems such as the eastern English Channel (region 3) and southern North Sea (region 2)
1753
1754 690 there was a thermally driven increase in pCO₂ to above atmospheric levels in summer. Non-
1755 691 thermal processes (such as mixing and the remineralisation of organic material) dominated in
1756
1757 692 winter, especially to the northwest of Scotland (region 6) and in Liverpool Bay (region 5). In
1758 693 all regions, the seawater pCO₂ was under-saturated in spring in respect to the atmospheric
1759
1760 694 equilibrium. In the well-mixed inner shelf regions pCO₂ was over-saturated for the rest of the
1761
1762 695 year whereas pCO₂ remained under-saturated throughout the year in the seasonally stratified
1763 696 regions such as the Celtic sea (region 4). The seasonal variations in under and over saturation
1764
1765 697 of pCO₂ will have implications in calculations of shelf wide net CO₂ flux, presented and

1771
1772
1773 698 discussed in Kitidis et al., (in prep., 2018). TA concentrations remained relatively constant
1774
1775 699 seasonally and showed a similar distribution to salinity, as both are influenced in part by
1776
1777 700 evaporation and precipitation. However, the lowest TA and lowest pH values were observed at
1778
1779 701 the end of winter in the northern North Sea (region 1). We have shown that calcite saturation
1780
1781 702 values are currently above 1.0 in all regions and such results will be useful for studies of ocean
1782
1783 703 acidification in the future.

1783 704 This synthesis provided a 18 month ‘snapshot’ of the diverse and dynamic ecosystems
1784
1785 705 around the northwest European shelf. It is complicated to catch the variability of complex
1786
1787 706 ecosystems as the ecohydrodynamic regions studied were very diverse and dynamic. Within
1788
1789 707 each region further subdivisions were identified and the seasonal variation in biogeochemistry
1790
1791 708 within these regions will have implications for using such broad hydrographic divisions to
1792
1793 709 study biogeochemical variations on the northwest European shelf. Incorporating high
1794
1795 710 frequency underway data (as was available for pCO₂ measurements) improved both the
1796
1797 711 seasonal and spatial coverage over what was possible with bottle sampling alone. Generally,
1798
1799 712 the wintertime period was under sampled, as were some regions year round, including the
1800
1801 713 Norwegian Trench (region 9) and the Minches (region 6). Addressing these issues could be the
1802
1803 714 focus for further sampling campaigns. The increased use of autonomous measurements on
1804
1805 715 robust platforms (such as buoys and autonomous surface vehicles) would help in this regard.

1802 716 The data have sufficient coherence and breadth of coverage to develop models that
1803
1804 717 would link physical and biogeochemical processes. The SSB data set could also be used to
1805
1806 718 extend existing studies to create a time series. Once we have a longer time series, we could
1807
1808 719 use this data set to quantify trends in pH and pCO₂, so we recommend that the sampling
1809
1810 720 continue to quantify year-to-year variability and elucidate trends in the data. In conclusion, the
1811
1812 721 large database collected as part of the shelf wide sampling within the SSB project will improve
1813
1814 722 the understanding of carbonate chemistry in relation to nutrient biogeochemistry over the
1815
1816 723 North-Western European Shelf, particularly in the context of climate change and ocean
1817
1818 724 acidification.

1819 726 **Acknowledgements**

1821 727 This study was supported by the UK NERC and DEFRA funded Shelf Sea
1822
1823 728 Biogeochemistry strategic research programme, NOC grant reference number NE/K001701/1;
1824
1825 729 PML grant reference NE/K002058/1; Cefas grant number NE/K001957/1; University of

1830
1831
1832
1833
1834
1835
1836
1837
1838
1839
1840
1841
1842
1843
1844
1845
1846
1847
1848
1849
1850
1851
1852
1853
1854
1855
1856
1857
1858
1859
1860
1861
1862
1863
1864
1865
1866
1867
1868
1869
1870
1871
1872
1873
1874
1875
1876
1877
1878
1879
1880
1881
1882
1883
1884
1885
1886
1887
1888

730 Southampton reference NE/K00185X/1. We would like to thank all of our samplers and cruise
731 participants plus the many people involved in rerouting the frozen samples as required. We are
732 also indebted to all scientific staff, crew and officers on board the many ships and campaigns
733 involved in this study. We are very grateful to the two anonymous reviewers who have added
734 substantially to the interpretation. All of the SSB shelf wide sampling data are publicly
735 available through BODC <http://www.uk-ssb.org/data/> and as listed in the references.

736

737 **References**

738 Artioli, Y., Blackford, J.C., Nondal, G., Bellerby, R.G.J., Wakelin, S.L., Holt, J.T., Butenschön,
739 M., Allen, J.I., 2014. Heterogeneity of impacts of high CO₂ on the North Western
740 European shelf. *Biogeosciences*, 11, 601–612.

741 Anderson, L.A. and Sarmiento, J.L., 1994. Redfield ratios of remineralization determined by
742 nutrient data analysis. *Global biogeochemical cycles*, 8(1), pp.65-80.

743 Bates, N., Astor, Y., Church, M., Currie, K., Dore, J., Gonaález-Dávila, M., Lorenzoni, L.,
744 Muller-Karger, F., Olafsson, J. and Santa-Casiano, M., 2014. A time view of changing
745 ocean chemistry due to ocean uptake of anthropogenic CO₂ and ocean
746 acidification. *Oceanography*, 27(1), pp.126-141.

747 Beare D, McQuatters-Gollop A, van der Hammen T, Machiels M, Teoh S.J., 2013. Long-Term
748 Trends in Calcifying Plankton and pH in the North Sea. *PLoS ONE* 8(5): e61175.
749 doi:10.1371/journal.pone.0061175

750 Borges, A., 2005. Do we have enough pieces of the jigsaw to integrate CO₂ fluxes in the coastal
751 ocean? *Estuaries and Coasts* 28(1), 3–27.

752 Bresnan, E., Cook, K.B., Hughes, S.L., Hay, S.J., Smith, K., Walsham, P. and Webster, L.,
753 2015. Seasonality of the plankton community at an east and west coast monitoring site
754 in Scottish waters. *Journal of Sea Research*, 105, pp.16-29.

755 Brewer, P.G. and Riley, J.P., 1965, December. The automatic determination of nitrate in sea
756 water. In *Deep Sea Research and Oceanographic Abstracts* (Vol. 12, No. 6, pp. 765-
757 772). Elsevier.

758 Brewer, P.G. and Goldman, J.C., 1976. Alkalinity changes generated by phytoplankton growth.
759 *Limnology and Oceanography*, 21(1): 108-117.

760 Cai, W.-J., 2011. Estuarine and Coastal Ocean Carbon Paradox : CO₂ Sinks or Sites of
761 Terrestrial Carbon Incineration. *Annual Review of Marine Science* 3, 123–145.

1889
1890
1891
1892
1893
1894
1895
1896
1897
1898
1899
1900
1901
1902
1903
1904
1905
1906
1907
1908
1909
1910
1911
1912
1913
1914
1915
1916
1917
1918
1919
1920
1921
1922
1923
1924
1925
1926
1927
1928
1929
1930
1931
1932
1933
1934
1935
1936
1937
1938
1939
1940
1941
1942
1943
1944
1945
1946
1947

762 Caldeira, K. and Wickett, M.E., 2003. Oceanography: anthropogenic carbon and ocean pH.
763 Nature, 425(6956), pp.365-365.

764 Chen, C.T.A. and Borges, A.V., 2009. Reconciling opposing views on carbon cycling in the
765 coastal ocean: continental shelves as sinks and near-shore ecosystems as sources of
766 atmospheric CO₂. Deep Sea Research Part II: Topical Studies in Oceanography, 56(8),
767 pp.578-590.

768 Cushing, O.M., 1973. Productivity of the North Sea. In: E.D. Goldberg {Editor}, North Sea
769 Science. MIT Press, Cambridge, MA.

770 Dickson, A.G. and Millero, F.J., 1987. A comparison of the equilibrium constants for the
771 dissociation of carbonic acid in seawater media. Deep Sea Research Part A.
772 Oceanographic Research Papers, 34(10), pp.1733-1743.

773 Dickson, A.G., Afghan, J.D. and Anderson, G.C., 2003. Reference materials for oceanic CO₂
774 analysis: a method for the certification of total alkalinity. Marine Chemistry, 80(2),
775 pp.185-197.

776 Dickson, A.G., Sabine, C.L. and Christian, J.R., 2007. Guide to best practices for ocean CO₂
777 measurements.

778 Doney, S.C., Fabry, V.J., Feely, R. A., Kleypas, J.A., 2009. Ocean Acidification: The Other
779 CO₂ Problem. Annual Review of Marine Science 1, 169–192.

780 Doney, S.C., Ruckelshaus, M., Duffy, J.E., Barry, J.P., Chan, F., English, C.A., Galindo, H.M.,
781 Grebmeier, J.M., Hollowed, A.B., Knowlton, N. and Polovina, J., 2011. Climate change
782 impacts on marine ecosystems. Ann. Rev. Mar. Sci. 4 (1), 11–37.
783 <http://dx.doi.org/10.1146/annurev-marine-041911-111611>.

784 Duarte, C.M., Hendriks, I.E., Moore, T.S., Olsen, Y.S., Steckbauer, A., Ramajo, L., Carstensen,
785 J., Trotter, J.A. and McCulloch, M., 2013. Is ocean acidification an open-ocean
786 syndrome? Understanding anthropogenic impacts on seawater pH. Estuaries and Coasts,
787 36(2), pp.221-236.

788 Egleston, E.S., Sabine, C.L. and Morel, F.M., 2010. Revelle revisited: Buffer factors that
789 quantify the response of ocean chemistry to changes in DIC and alkalinity. Global
790 Biogeochemical Cycles, 24(1) GB1002, doi:10.1029/2008gb003407

791 Fabry, V.J., Seibel, B.A., Feely, R.A. and Orr, J.C., 2008. Impacts of ocean acidification on
792 marine fauna and ecosystem processes. ICES Journal of Marine Science, 65(3), pp.414-
793 432.

794 Feely, R.A., Doney, S.C., Cooley, S.R., 2009. Ocean acidification: present conditions and

1948
1949
1950
1951
1952
1953
1954
1955
1956
1957
1958
1959
1960
1961
1962
1963
1964
1965
1966
1967
1968
1969
1970
1971
1972
1973
1974
1975
1976
1977
1978
1979
1980
1981
1982
1983
1984
1985
1986
1987
1988
1989
1990
1991
1992
1993
1994
1995
1996
1997
1998
1999
2000
2001
2002
2003
2004
2005
2006

795 future changes in a high-CO₂ world. *Oceanography* 22 (4), 36–47.

796 Frankignoulle, M., Bourge, I., Canon, C. and Dauby, P., 1996. Distribution of surface seawater
797 partial CO₂ pressure in the English Channel and in the Southern Bight of the North Sea.
798 *Continental Shelf Research*, 16(3), pp.381-395.

799 Frigstad, H., Henson, S.A., Hartman, S.E., Omar, A.M., Jeansson, E., Cole, H., Pebody, C. and
800 Lampitt, R.S., 2015. Links between surface productivity and deep ocean particle flux
801 at the Porcupine Abyssal Plain (PAP) sustained observatory. *Biogeosciences*, 12(6).

802 Froelich, P., Klinkhammer, G.P., Bender, M.A.A., Luedtke, N.A., Heath, G.R., Cullen, D.,
803 Dauphin, P., Hammond, D., Hartman, B. and Maynard, V., 1979. Early oxidation of
804 organic matter in pelagic sediments of the eastern equatorial Atlantic: suboxic
805 diagenesis. *Geochimica et Cosmochimica Acta*, 43(7), pp.1075-1090.

806 Garcia-Soto, C. and Pingree, R.D., 1998. Late autumn distribution and seasonality of
807 chlorophyll-a at the shelf-break/slope region of the Armorican and Celtic Shelf. *Journal*
808 *of the Marine Biological Association of the United Kingdom*, 78(1), pp.17-33.

809 Gattuso, J.P., and L. Hansson, 2011. *Ocean Acidification*. Oxford University Press, Oxford UK,
810 eds., 326 pp.

811 Gerlach S. A., 1988. Nutrients--an overview. In *Environmental Protection of the North Sea*
812 (edited by Newman P. J. and Agg A. R.), pp. 147-175. Heinemann, Oxford.

813 Gowen, R.J., Hydes, D.J., Mills, D.K., Stewart, B.M., Brown, J., Gibson, C.E., Shammon, T.M.,
814 Allen, M., Malcolm, S.J., 2002. Assessing trends in nutrient concentrations in coastal
815 shelf seas: a case study in the Irish Sea. *Estuarine, Coastal and Shelf Science* 54,
816 927e939.

817 Gowen, R.J., Tett, P., Kennington, K., Mills, D.K., Shammon, T.M., Stewart, B.M.,
818 Greenwood, N., Flanagan, C., Devlin, M. and Wither, A., 2008. The Irish Sea: is it
819 eutrophic?. *Estuarine, Coastal and Shelf Science*, 76(2), pp.239-254.

820 Greenwood, N., Hydes, D.J., Mahaffey, C., Wither, A., Barry, J., Sivyer, D.B., Pearce, D.J.,
821 Hartman, S.E., Andres, O. and Lees, H.E., 2011. Spatial and temporal variability in
822 nutrient concentrations in Liverpool Bay, a temperate latitude region of freshwater
823 influence. *Ocean Dynamics*, 61(12), pp.2181-2199.

824 Gruber N, Galloway JN. 2008. An earth-system perspective of the global nitrogen cycle. *Nature*
825 451: 293–296

826 Harlay, J., Borges, A.V., Van Der Zee, C., Delille, B., Godoi, R.H.M., Schiettecatte, L.S.,
827 Roevros, N., Aerts, K., Lapernat, P.E., Rebreanu, L. and Groom, S., 2010.

2007
2008
2009
2010
2011
2012
2013
2014
2015
2016
2017
2018
2019
2020
2021
2022
2023
2024
2025
2026
2027
2028
2029
2030
2031
2032
2033
2034
2035
2036
2037
2038
2039
2040
2041
2042
2043
2044
2045
2046
2047
2048
2049
2050
2051
2052
2053
2054
2055
2056
2057
2058
2059
2060
2061
2062
2063
2064
2065

828 Biogeochemical study of a coccolithophore bloom in the northern Bay of Biscay (NE
Atlantic Ocean) in June 2004. *Progress in Oceanography*, 86(3), pp.317-336.

830 Hartman S.E., Kivimae C., Salt L., Clargo N.M., 2017. Dissolved Inorganic Carbon and Total
Alkalinity from cruise DY017 to the Hebrides Shelf (55-60°N, 6-10°W). *British
Oceanographic Data Centre - Natural Environment Research Council, UK.* doi:10/b83q.

833 Henson, S.A., Sanders, R., Allen, J.T., Robinson, I.S. and Brown, L., 2003. Seasonal
constraints on the estimation of new production from space using temperature-nitrate
relationships. *Geophysical Research Letters*, 30(17).

836 Henson, S.A., Beulieu, C. & Lampitt, R. 2016. Observing climate change trends in ocean
biogeochemistry: when and where. *Global Change Biology*, 22, 1561–1571, doi:
10.1111/gcb.13152

839 Hoppe, C.J.M., G. Langer, S. D. Rokitta, D.A. Wolf-Gladrow, and B. Rost., 2012. Implications
of observed inconsistencies in carbonate chemistry measurements for ocean
acidification studies. *Biogeosciences* 9, 2401-2405.

842 Howarth, R.W., Billen, G., Swaney, D., Townsend, A., Jaworski, N., Lajtha, K., Downing, J.A.,
Elmgren, R., Caraco, N., Jordan, T. and Berendse, F., 1996. Regional nitrogen budgets
and riverine N & P fluxes for the drainages to the North Atlantic Ocean: Natural and
human influences. In *Nitrogen cycling in the North Atlantic Ocean and its watersheds*
(pp. 75-139). Springer Netherlands.

847 Humphreys, M.P., 2015. Calculating seawater total alkalinity from open-cell titration data
using a modified Gran plot technique, in: *Measurements and Concepts in Marine
Carbonate Chemistry*. PhD Thesis, Ocean and Earth Science, University of
Southampton, UK, pp. 25–44.

851 Humphreys, M.P., Achterberg, E.P., Hopkins, J.E., Chowdhury, M.Z.H., Griffiths, A.M.,
Hartman, S.E., Hull, T., Smilenova, A., Wihsgott, J.U., Woodward, E.M.S., Moore,
C.M., 2017. Mechanisms for a nutrient-conserving carbon pump in a seasonally
stratified, temperate continental shelf sea. *Prog. Oceanogr.* (in review).

855 Humphreys M.P., Griffiths A.M., Hartman S.E., Kivimae C., Achterberg E.P., 2017a. Seawater
dissolved inorganic carbon and total alkalinity for UK Shelf Sea Biogeochemistry
cruise DY026A. *British Oceanographic Data Centre - Natural Environment Research
Council, UK.* doi:10.5285/554b6d39-7fcc-260b-e053-6c86abc0733a.

859 Humphreys M.P., Griffiths A.M., Hartman S.E., Kivimae C., Achterberg E.P., 2017b. Seawater
dissolved inorganic carbon and total alkalinity for UK Shelf Sea Biogeochemistry

2066
2067
2068
2069
2070
2071
2072
2073
2074
2075
2076
2077
2078
2079
2080
2081
2082
2083
2084
2085
2086
2087
2088
2089
2090
2091
2092
2093
2094
2095
2096
2097
2098
2099
2100
2101
2102
2103
2104
2105
2106
2107
2108
2109
2110
2111
2112
2113
2114
2115
2116
2117
2118
2119
2120
2121
2122
2123
2124

861 cruise DY026B. British Oceanographic Data Centre - Natural Environment Research
862 Council, UK. doi:10.5285/554b6d39-7fcd-260b-e053-6c86abc0733a.

863 Humphreys M.P., Smilenova A., Poulton A., Hartman S.E., Kivimae C., Achterberg E.P.,
864 2017c. Seawater dissolved inorganic carbon and total alkalinity for UK Shelf Sea
865 Biogeochemistry cruise DY030. British Oceanographic Data Centre - Natural
866 Environment Research Council, UK. doi:10.5285/554b6d39-7fce-260b-e053-
867 6c86abc0733a.

868 Humphreys M.P., Smilenova A., Ruhl H., Hartman S.E., Kivimae C., Achterberg E.P., 2017d.
869 Seawater dissolved inorganic carbon and total alkalinity for UK Shelf Sea
870 Biogeochemistry cruise DY034. British Oceanographic Data Centre - Natural
871 Environment Research Council, UK. doi:10.5285/554b6d39-7fcf-260b-e053-
872 6c86abc0733a.

873 Humphreys M.P., Chowdhury M.Z.H., Griffiths A.M., Smilenova A., Clarke J., Greenwood
874 N., Hartman S.E., Kivimae C., Achterberg E.P., 2017e. Seawater dissolved inorganic
875 carbon and total alkalinity for UK Shelf Sea Biogeochemistry collected by the Centre
876 for Environment, Fisheries and Aquaculture Science British Oceanographic Data
877 Centre - Natural Environment Research Council, UK. doi:10.5285/5a52512d-54cb-
878 0f3a-e053-6c86abc085ba.

879 Humphreys M.P., Smilenova A., McGrath T., McGovern E., Hartman S.E., Kivimae C.,
880 Achterberg E.P., 2017f. Seawater dissolved inorganic carbon and total alkalinity for
881 UK Shelf Sea Biogeochemistry cruise CE15003 British Oceanographic Data Centre -
882 Natural Environment Research Council, UK. doi:10.5285/5a533687-7f7c-24e2-e053-
883 6c86abc0ea64.

884 Humphreys M.P., Clarke J., Walsham P., Hartman S.E., Kivimae C., Achterberg E.P., 2017g.
885 Seawater dissolved inorganic carbon and total alkalinity for UK Shelf Sea
886 Biogeochemistry collected by Marine Scotland Science British Oceanographic Data
887 Centre - Natural Environment Research Council, UK. doi:10.5285/5a533687-7f7d-
888 24e2-e053-6c86abc0ea64.

889 Humphreys M.P., Chowdhury M.Z.H., Griffiths A.M., Smilenova A., Stewart B., Hartman S.E.,
890 Kivimae C., Achterberg E.P., 2017h. Seawater dissolved inorganic carbon and total
891 alkalinity for UK Shelf Sea Biogeochemistry collected by Agri-Food and Biosciences
892 Institute British Oceanographic Data Centre - Natural Environment Research Council,
893 UK. doi:10.5285/5a533687-7f7b-24e2-e053-6c86abc0ea64.

2125
2126
2127 894 Huthnance, J.M., 1995. Circulation, exchange and water masses at the ocean margin: the role
2128 of physical processes at the shelf edge. *Progress in Oceanography*, 35(4), pp.353-431.
2129 895
2130 Huthnance, J.M., 1997. North Sea interaction with the North Atlantic ocean. *Deutsche*
2131 *Hydrografische Zeitschrift*, 49(2-3), pp.153-162.
2132 897
2133 Huthnance, J.M., Holt, J.T. and Wakelin, S.L., 2009. Deep ocean exchange with west-
2134 European shelf seas. *Ocean Science*, 5(4), pp.621-634.
2135 899
2136 Hydes, D.J., Kelly-Gerreyn, B.A., Le Gall, A.C. and Proctor, R., 1999. The balance of supply
2137 900 of nutrients and demands of biological production and denitrification in a temperate
2138 901 latitude shelf sea—a treatment of the southern North Sea as an extended estuary. *Marine*
2139 902 *Chemistry*, 68(1), pp.117-131.
2140 903
2141 Hydes, D.J., Gowen, R.J., Holliday, N.P., Shammon, T. and Mills, D., 2004. External and
2142 904 internal control of winter concentrations of nutrients (N, P and Si) in north-west
2143 905 European shelf seas. *Estuarine, Coastal and Shelf Science*, 59(1), pp.151-161.
2144 906
2145 Hydes, D J, Aoyama M, Aminot A, Bakker K, Becker S, Coverly S, Daniel A, Dickson a G,
2146 907 Grosso O, Kerouel R, van Ooijen J, Sato K, Tanhua T, Woodward E M S, Zhang J Z.
2147 908 2010. Determination of dissolved nutrients (N,P,Si) in seawater with high precision and
2148 909 inter-comparability using gas-segmented continuous flow analysers. The GO-SHIP
2149 910 Repeat Hydrography Manual: a collection of expert reports and guidelines; IOCCP
2150 911 report No.14, ICPO publication series No. 134, version 1.
2151 912
2152 Hydes, D. J., Hartman S.E., Hartman M.C., Jiang Z., Hardman-Mountford N., Artioli Y.,
2153 913 Blackford J., Litt E., and Schuster U., 2011. DEFRApH, Tech. rep. DEFRA contract
2154 914 ME4133 “DEFRApH monitoring project”. Southampton, UK, National Oceanography
2155 915 Centre Southampton, 53 pp. National Oceanography Centre Southampton Research and
2156 916 Consultancy
2157 917
2158 Hydes, D.J. and Hartman, S.E., 2012. Seasonal and inter-annual variability in alkalinity in
2159 918 Liverpool Bay (53.5° N, 3.5° W) and in major river inputs to the North Sea. *Ocean*
2160 919 *Dynamics*, 62(2), pp.321-333.
2161 920
2162 Jiang, Z.P., Hydes, D.J., Tyrrell, T., Hartman, S.E., Hartman, M.C., Dumousseaud, C., Padin,
2163 921 X.A., Skjelvan, I. and González-Pola, C., 2013. Key controls on the seasonal and
2164 922 interannual variations of the carbonate system and air-sea CO₂ flux in the Northeast
2165 923 Atlantic (Bay of Biscay). *Journal of Geophysical Research: Oceans*, 118(2), pp.785-800.
2166 924
2167 Jiang, Z.P., Tyrrell, T., Hydes, D.J., Dai, M. and Hartman, S.E., 2014. Variability of alkalinity
2168 925 and the alkalinity-salinity relationship in the tropical and subtropical surface ocean.
2169 926

2184
2185
2186 927 Global Biogeochemical Cycles, 28(7), pp.729-742.
2187
2188 928 Johnston, R., 1973. Nutrients and metals in the North Sea. North Sea Science., pp.293-307.
2189
2190 929 Kirkwood, D.S., 1989. Simultaneous determination of selected nutrients in sea water.
2191 930 International Council for the Exploration of the Sea. ICES CM 1989/C:29.
2192
2193 931 Simultaneous determination of selected nutrients in sea water.
2194 932 Kitidis, V., Hardman-Mountford, N.J., Litt, E., Brown, I., Cummings, D., Hartman, S., Hydes,
2195 933 D., Fishwick, J.R., Harris, C., Martinez-Vicente, V. and Woodward, E.M.S., 2012.
2196 934 Seasonal dynamics of the carbonate system in the Western English Channel.
2197 935 Continental Shelf Research, 42, pp.30-40.
2198
2199 936 Kitidis, V., Tait, K., Nunes, J., Brown, I., Woodward, E.M.S., Harris, C., Sabadel, A.J.M.,
2200 937 Sivyer, D.B., Silburn, B. and Kröger, S., 2017. Seasonal benthic nitrogen cycling in a
2201 938 temperate shelf sea: the Celtic Sea. Biogeochemistry, pp.1-17.
2202
2203 939 Kitidis V, Shutler J.D., Ashton I., Warren M. , Brown I. , Findlay H. , Hartman S.E. ,
2204 940 Humphreys M. , Kivimäe C. , Greenwood N. , Hull T. , Pearce D. , McGrath T. , Stewart
2205 941 B.M., Walsham P., McGovern E., Bozec Y., Gac, J-P., vanHeuven S., Hoppema M.,
2206 942 Schuster U. , Johannessen T., Omar A., Lauvset S., Skjelvan I., Olsen A., Steinhoff T.,
2207 943 Körtzinger A., Becker M., Lefevre N., Gkritzalis T., Catrijsee A., Petersen W.,
2208 944 Voynova Y., Chapron, B., Grouazel, A. , Land, P. E. , Nightingale P.D. , 2018. (in
2209 945 prep.), GRL.
2210
2211 946 Koeve, W., Oschlies, A., 2012. Potential impact of DOM accumulation on fCO₂ and carbonate
2212 947 ion computations in ocean acidification experiments. Biogeosciences 9, 3787–3798.
2213
2214 948 Körtzinger, A., Send, U., Lampitt, R.S., Hartman, S., Wallace, D.W., Karstensen, J.,
2215 949 Villagarcia, M.G., Llinás, O. and DeGrandpre, M.D., 2008. The seasonal pCO₂ cycle
2216 950 at 49 N/16.5 W in the northeastern Atlantic Ocean and what it tells us about biological
2217 951 productivity. Journal of Geophysical Research: Oceans, 113(C4).
2218
2219 952 Laruelle, G.G., Lauerwald, R., Pfeil, B. and Regnier, P., 2014. Regionalized global budget of
2220 953 the CO₂ exchange at the air-water interface in continental shelf seas. Global
2221 954 biogeochemical cycles, 28(11), pp.1199-1214.
2222
2223 955 Lee, K., Tong, L.T., Millero, F.J., Sabine, C.L., Dickson, A.G., Goyet, C., Park, G.H.,
2224 956 Wanninkhof, R., Feely, R.A. and Key, R.M., 2006. Global relationships of total
2225 957 alkalinity with salinity and temperature in surface waters of the world's oceans.
2226 958 Geophysical Research Letters, 33(19).
2227
2228 959 Lewis, E., Wallace, D. and Allison, L.J., 1998. Program developed for CO₂ system calculations

2243
2244
2245
2246
2247
2248
2249
2250
2251
2252
2253
2254
2255
2256
2257
2258
2259
2260
2261
2262
2263
2264
2265
2266
2267
2268
2269
2270
2271
2272
2273
2274
2275
2276
2277
2278
2279
2280
2281
2282
2283
2284
2285
2286
2287
2288
2289
2290
2291
2292
2293
2294
2295
2296
2297
2298
2299
2300
2301

960 (p. 38). Tennessee: Carbon Dioxide Information Analysis Center, managed by
961 Lockheed Martin Energy Research Corporation for the US Department of Energy

962 L'Helguen, S., C. Madec, and P. Le Corre, 1996. Nitrogen uptake in permanently well-mixed
963 temperate coastal waters. *Estuarine Coastal Shelf Sci.*, 42, 803-818.

964 Liu, K.K., Atkinson, L., Quiñones, R.A. and Talaue-McManus, L., 2010. Biogeochemistry of
965 continental margins in a global context. In *Carbon and Nutrient Fluxes in Continental
966 Margins* (pp. 3-24). Springer Berlin Heidelberg.

967 Marrec, P., Cariou, T., Collin, E., Durand, A., Latimier, M., Macé, E., Morin, P., Raimund, S.,
968 Vernet, M. and Bozec, Y., 2013. Seasonal and latitudinal variability of the CO₂ system
969 in the western English Channel based on Voluntary Observing Ship (VOS)
970 measurements. *Marine Chemistry*, 155, pp.29-41.

971 Marrec, P., Cariou, T., Macé, E., Morin, P., Salt, L. A., Vernet, M., Taylor, B., Paxman, K.,
972 and Bozec, Y., 2015. Dynamics of air–sea CO₂ fluxes in the northwestern European
973 shelf based on voluntary observing ship and satellite observations, *Biogeosciences*, 12,
974 5371-5391, doi:10.5194/bg-12-5371-2015.

975 McGrath T., McGovern E., Cave R.R., Kivimäe C., 2016. The Inorganic Carbon Chemistry in
976 Coastal and Shelf Waters around Ireland. *Estuaries and Coasts*. 1-13.

977 Millero, F. J., Dickson, A. G., Eiseheid, G., Goyet, C., Guenther, P., Johnson, K. M., Key, R.
978 M., Lee, K., Purkenson, D., Sabine, C. L., Schottle, R. G., Wallace, D. W. R., Lewis,
979 E., and Winn, C. D., 1998. Assessment of the quality of the shipboard measurements
980 of total alkalinity on the WOCE Hydrographic Program Indian Ocean CO₂ survey
981 cruises 1994–1996, *Mar. Chem.*, 63, 9–20.

982 Millero, F.J., Pierrot, D., Lee, K., Wanninkhof, R., Feely, R., Sabine, C.L., Key, R.M.,
983 Takahashi, T., 2002. Dissociation constants for carbonic acid determined from field
984 measurements. *Deep Sea Res. I Oceanogr. Res. Pap.* 49 (10), 1705–1723.

985 Nelissen, P. H. M. & Stefels, J., 1988. Eutrophication in the North Sea. *NIOZ-Rapp.* I988-4, 1-100.

986 Ostle C., P. Williamson, Y. Artioli, D. C. E. Bakker, S. Birchenough, C. E. Davis, S. Dye, M.
987 Edwards, H. S. Findlay, N. Greenwood, S. Hartman, M. P. Humphreys, T. Jickells, M.
988 Johnson, P. Landschützer, R. Parker, D. Pearce, J. Pinnegar, C. Robinson, U. Schuster,
989 B. Silburn, R. Thomas, S. Wakelin, P. Walsham, and A. J. Watson., 2016. Carbon
990 dioxide and ocean acidification observations in UK waters: Synthesis report with a
991 focus on 2010- 2015. doi: 10.13140/RG.2.1.4819.4164.

992 Painter, S.C., Hartman, S.E., Kivimäe, C., Salt, L.A., Clargo, N.M., Bozec, Y., Daniels, C.J.,

2302
2303
2304 993 Jones, S.C., Hemsley, V.S., Munns, L.R. and Allen, S.R., 2016. Carbon exchange
2305 between a shelf sea and the ocean: The Hebrides Shelf, west of Scotland. *Journal of*
2306 994 *Geophysical Research: Oceans*, 121(7), pp.4522-4544.
2307 995
2308 996 Painter, S.C., Hartman, S.E., Kivimäe, C., Salt, L.A., Clargo, N.M., Daniels, C.J., Bozec, Y.,
2309 997 Daniels, L., Allen, S., Hemsley, V.S. and Moschonas, G., 2017. The elemental
2310 998 stoichiometry (C, Si, N, P) of the Hebrides Shelf and its role in carbon export. *Progress*
2311 999 *in Oceanography*, 159, pp.154-177.
2312 1000 Park, K.P., 1969. Oceanic CO₂ System: An evaluation of ten methods of investigation. *Limnol.*
2313 1001 *Oceanogr.* 14, 179-186.
2314 1002 Pingree, R. D., Pugh, P. R., Holligan, P. M., Forster, G. R., 1975. Summer phytoplankton
2315 1003 blooms and red tides along tidal fronts in the approaches to the English Channel, *Nature*,
2316 1004 258, 672-677.
2317 1005 Pingree, R. D. and Griffiths, D. K., 1978. Tidal fronts on the shelf seas around the British Isles,
2318 1006 *J. Geophys. Res.*, 83, 4615-4622.
2319 1007 Pingree, R.D., 1993. Flow of surface waters to the west of the British Isles and in the Bay of
2320 1008 Biscay. *Deep Sea Research Part II: Topical Studies in Oceanography*, 40(1-2), pp.369-
2321 1009 388. Provoost, P., Heuven, S.V., Soetaert, K., Laane, R.W.P.M. and Middelburg, J.J.,
2322 1010 2010. Seasonal and long-term changes in pH in the Dutch coastal zone. *Biogeosciences*,
2323 1011 7(11), pp.3869-3878.
2324 1012 Radach, G. and Moll, A., 1993. Estimation of the variability of production by simulating annual
2325 1013 cycles of phytoplankton in the central North Sea. *Progress in Oceanography*, 31(4),
2326 1014 pp.339-419.
2327 1015 Redfield, A.C., Ketchum, B.H. and Richards, E.A., 1963. The influence of organisms on the
2328 1016 composition of sea water. *The sea*, pp.26-77.
2329 1017 Ribas-Ribas, M., Rerolle, V., Bakker, D.C., Kitidis, V., Lee, G., Brown, I., Achterberg, E.P.,
2330 1018 Hardman-Mountford, N. and Tyrrell, T., 2014. Intercomparison of carbonate chemistry
2331 1019 measurements on a cruise in northwestern European shelf seas. *Biogeosciences*, 11,
2332 1020 pp.4339-4355.
2333 1021 Riebesell, U. and Tortell, P.D., 2011. Effects of ocean acidification on pelagic organisms and
2334 1022 ecosystems. *Ocean acidification*. Oxford University Press, Oxford, pp.99-121.
2335 1023 Salt, L.A., Thomas, H., Prowe, A.E., Borges, A.V., Bozec, Y. and Baar, H.J., 2013. Variability
2336 1024 of North Sea pH and CO₂ in response to North Atlantic Oscillation forcing. *Journal of*
2337 1025 *Geophysical Research: Biogeosciences*, 118(4), pp.1584-1592.
2338
2339
2340
2341
2342
2343
2344
2345
2346
2347
2348
2349
2350
2351
2352
2353
2354
2355
2356
2357
2358
2359
2360

2361
2362
2363 1026 Salt, L.A., Thomas, H., Bozec, Y., Borges, A.V. and De Baar, H.J., 2016. The internal
2364 consistency of the North Sea carbonate system. *Journal of Marine Systems*, 157, pp.52-
2365 1027 64.
2366
2367 1028
2368 1029 Sambrotto, R.N., Savidge, G., Robinson, C., Boyd, P., Takahashi, T., Karl, D.M., Langdon, C.,
2369 Chipman, D., Marra, J. and Codispoti, L., 1993. Elevated consumption of carbon
2370 1030 relative to nitrogen in the surface ocean. *Nature*, 363(6426), pp.248-250.
2371 1031
2372
2373 1032 Sarmiento, J.L. and Gruber, N., 2006. *Ocean biogeochemical cycles*. Princeton University.
2374
2375 1033 Sathyendranath, S. and Platt, T., 1991. Estimation of new production in the ocean by compound
2376 1034 remote sensing. *Nature*, 353(6340), p.129.
2377
2378 1035 Seitzinger, S.P., Giblin, A.E., 1996. Estimating denitrification in the North Atlantic continental
2379 1036 shelf sediments. *Biogeochemistry* 35, 235-260.
2380
2381 1037 Shadwick, E. H., Thomas, H., Azetsu-Scott, K., Greenan, B. J. W., Head, E., and Horne, E.,
2382 1038 2011. Seasonal variability of dissolved inorganic carbon and surface water pCO₂ in the
2383 Scotian Shelf region of the Northwestern Atlantic, *Mar. Chem.*, 124, 23–37,
2384 1039 doi:10.1016/j.marchem.2010.11.004.
2385
2386 1040
2387 1041 Siegel, D.A., Doney, S.C. and Yoder, J.A., 2002. The North Atlantic spring phytoplankton
2388 bloom and Sverdrup's critical depth hypothesis. *Science*, 296(5568), pp.730-733.
2389 1042
2390 1043 Simpson, J.H., Hunter, J.R, 1974. Fronts in the Irish Sea, *Nature*, 250, 404-406.
2391
2392 1044 Smith, A.F., Fryer, R.J., Webster, L., Berx, B., Taylor, A., Walsham, P. and Turrell, W.R.,
2393 1045 2014. Setting background nutrient levels for coastal waters with oceanic influences.
2394 *Estuarine, Coastal and Shelf Science*, 145, pp.69-79.
2395 1046
2396
2397 1047 Smyth, T.J., Fishwick, J.R., Lisa, A.M., Cummings, D.G., Harris, C., Kitidis, V., Rees, A.,
2398 1048 Martinez-Vicente, V. and Woodward, E.M., 2010. A broad spatio-temporal view of the
2399 Western English Channel observatory. *Journal of Plankton Research*, 32(5), pp.585-
2400 1049 601.
2401
2402 1050
2403 1051 Takahashi, T., Sutherland, S.C., Sweeney, C., Poisson, A., Metzl, N., Tilbrook, B., Bates, N.,
2404 Wanninkhof, R., Feely, R.A., Sabine, C. and Olafsson, J., 2002. Global sea-air CO₂
2405 1052 flux based on climatological surface ocean pCO₂, and seasonal biological and
2406 1053 temperature effects. *Deep Sea Research Part II: Topical Studies in Oceanography*, 49(9),
2407 1054 pp.1601-1622.
2408
2409
2410 1055
2411 1056 Thomas, H., Bozec, Y., Elkalay, K. and De Baar, H.J., 2004. Enhanced open ocean storage of
2412 CO₂ from shelf sea pumping. *Science*, 304(5673), pp.1005-1008.
2413 1057
2414 1058 Thomas, H., Bozec, Y., Elkalay, K., De Baar, H.J.W., Borges, A.V. and Schiettecatte, L.S.,
2415
2416
2417
2418
2419

2420
2421
2422 1059 2005. Controls of the surface water partial pressure of CO₂ in the North Sea.
2423 Biogeosciences, 2(4), pp.323-334.
2424 1060
2425 Thomas, H., Schiettecatte, L.S., Borges, A.V., Elkalay, K. and de Baar, H.J., 2006. Assessment
2426 1061 of the processes controlling seasonal variations of dissolved inorganic carbon in the
2427 1062 North Sea. *Limnology and Oceanography*, 51(6), pp.2746-2762.
2428
2429 1063 Thomas, H., Friederike Prowe, A.E., van Heuven, S., Bozec, Y., de Baar, H.J., Schiettecatte,
2430 1064 L.S., Suykens, K., Koné, M., Borges, A.V., Lima, I.D. and Doney, S.C., 2007. Rapid
2432 1065 decline of the CO₂ buffering capacity in the North Sea and implications for the North
2433 1066 Atlantic Ocean. *Global Biogeochemical Cycles*, 21(4).
2434
2435 1067 UKMMAS (2010). *Charting Progress 2- An Assessment of the State of UK seas*.
2436 1068
2438 1069 van Leeuwen, S., Tett, P., Mills, D. and van der Molen, J., 2015. Stratified and nonstratified
2439 1070 areas in the North Sea: Long-term variability and biological and policy implications.
2440 1071 *Journal of Geophysical Research: Oceans*, 120(7), pp.4670-4686.
2441
2442 1072 Waldbusser, G.G. and Salisbury, J.E., 2014. Ocean Acidification in the Coastal Zone from an
2443 1073 Organism's Perspective: Multiple System Parameters, Frequency Domains, and
2444 1074 Habitats. *Annual Review of Marine Sciences*, 6: 221-247.
2445
2446 1075 Wanninkhof, R., 2014. Relationship between wind speed and gas exchange over the ocean
2447 1076 revisited. *Limnology and Oceanography: Methods*, 12(6), pp.351-362.
2448
2449 1077 Waters, J.F. and Millero, F.J., 2013. The free proton concentration scale for seawater pH.
2450 1078 *Marine Chemistry*, 149, pp.8-22.
2451
2452 1079 Wolf-Gladrow, D.A., Zeebe, R.E., Klaas, C., Koertzing, A. and Dickson, A.G., 2007. Total
2453 1080 alkalinity: The explicit conservative expression and its application to biogeochemical
2454 1081 processes. *Marine Chemistry*, 106(1-2): 287-300.
2455
2456 1082 Zeebe R. E. and Wolf-Gladrow, D. A., 2001. CO₂ in seawater: equilibrium, kinetics, isotopes,
2457 1083 Elsevier Oceanography Series, 65, Amsterdam, 346 pp.
2458
2459 1084
2460
2461
2462
2463
2464
2465
2466
2467
2468
2469
2470
2471
2472
2473
2474
2475
2476
2477
2478

2479
2480
2481
2482
2483
2484
2485
2486
2487
2488
2489
2490
2491
2492
2493
2494
2495
2496
2497
2498
2499
2500
2501
2502
2503
2504
2505
2506
2507
2508
2509
2510
2511
2512
2513
2514
2515
2516
2517
2518
2519

1085 Table 1 a) The mean average (and standard deviation) for the hydrograph and nutrient data in winter (jan-mar), spring (apr-jun), summer (jul-sep)
1086 and autumn (oct-dec) for each of the 9 ecohydrographic regions (numbered 1-9). Where insufficient samples exist, n/a has been used.

1087

	Temperature (°C)				Practical salinity				Phosphate ($\mu\text{mol kg}^{-1}$)				Silicate ($\mu\text{mol kg}^{-1}$)				Nitrite ($\mu\text{mol kg}^{-1}$)			
	jan-mar	apr-jun	jul-sep	oct-dec	jan-mar	apr-jun	jul-sep	oct-dec	jan-mar	apr-jun	jul-sep	oct-dec	jan-mar	apr-jun	jul-sep	oct-dec	jan-mar	apr-jun	jul-sep	oct-dec
1	7.65	13.78	14.36	11.65	33.26	34.11	34.61	34.78	0.54	0.08	0.09	0.36	3.59	0.95	0.75	3.07	0.12	0.03	0.06	0.18
	(0.52)	(2.44)	(1.27)	(0.45)	(3.9)	(0.40)	(0.61)	(0.02)	(0.08)	(0.11)	(0.08)	(0.01)	(1.55)	(0.57)	(0.60)	(0.49)	(0.08)	(0.07)	(0.10)	(0.01)
2	7.86	12.40	17.69	14.24	34.08	34.56	34.43	34.67	0.35	0.10	0.16	0.50	2.13	0.80	1.92	3.72	0.14	0.02	0.10	0.59
	(0.85)	(1.27)	(1.67)	(1.28)	(1.53)	(0.36)	(0.42)	(0.34)	(0.12)	(0.07)	(0.13)	(0.44)	(1.48)	(0.53)	(1.77)	(2.13)	(0.10)	(0.05)	(0.15)	(0.46)
3	9.44	12.25	18.27	16.69	34.95	30.64	34.86	35.15	0.53	0.08	1.91	0.35	5.10	2.88	3.62	3.76	0.10	0.11	0.09	0.19
	(0.70)	(1.93)	(0.80)	(1.25)	(0.54)	(10.81)	(0.29)	(0.11)	(0.05)	(0.07)	(6.46)	(0.26)	(2.33)	(9.18)	(5.72)	(1.44)	(0.06)	(0.25)	(0.13)	(0.14)
4	9.48	11.32	16.63	15.84	35.22	35.27	34.12	33.39	0.53	0.21	0.09	0.27	4.23	2.14	0.80	2.27	0.10	0.07	0.08	0.23
	(0.57)	(1.56)	(2.68)	(5.89)	(0.14)	(0.17)	(4.42)	(6.43)	(0.12)	(0.16)	(0.16)	(0.23)	(0.90)	(0.93)	(1.17)	(1.62)	(0.08)	(0.05)	(0.29)	(0.17)
5	8.00	10.53	15.37	14.06	33.80	33.81	34.02	34.19	0.64	0.36	0.25	0.95	7.54	3.00	2.13	5.31	0.13	0.11	0.15	0.23
	(1.40)	(1.84)	(1.14)	(0.89)	(0.78)	(0.81)	(0.46)	(0.36)	(0.22)	(0.21)	(0.18)	(2.15)	(3.34)	(2.30)	(1.19)	(5.59)	(0.18)	(0.09)	(0.23)	(0.36)
6	9.35	12.14	12.47	n/a	34.45	34.00	34.24	n/a	0.53	0.19	0.24	n/a	4.53	1.29	1.43	n/a	0.06	0.10	0.25	n/a
	(0.39)	(0.73)	(0.35)	n/a	(0.09)	(0.35)	(0.16)	n/a	(0.02)	(0.12)	(0.03)	n/a	(0.32)	(0.78)	(0.39)	n/a	(0.01)	(0.07)	(0.18)	n/a
7	8.74	9.70	14.01	18.41	34.53	34.94	35.11	34.87	0.59	0.42	0.13	0.36	4.56	1.54	0.48	2.65	0.27	0.23	0.06	0.31
	(0.58)	(1.80)	(1.05)	(10.87)	(0.50)	(0.42)	(0.27)	(0.2)	(0.04)	(0.27)	(0.11)	(0.03)	(1.01)	(0.79)	(0.29)	(0.43)	(0.13)	(0.14)	(0.05)	(0.18)
8	9.88	11.31	16.16	14.12	35.39	35.65	35.54	35.58	0.62	0.43	0.10	n/a	3.30	2.25	0.36	n/a	0.07	0.17	0.04	n/a
	(0.15)	(1.49)	(1.69)	(0.39)	(0.04)	(0.99)	(0.15)	(0.00)	n/a	(0.18)	(0.07)	n/a	n/a	(1.39)	(0.17)	n/a	n/a	(0.06)	(0.05)	n/a
9	n/a	10.75	14.03	n/a	n/a	34.26	34.65	n/a	n/a	0.17	0.04	n/a	n/a	1.29	0.42	n/a	n/a	0.16	0.01	n/a
	n/a	(1.91)	(0.80)	n/a	n/a	(0.61)	(0.43)	n/a	n/a	(0.14)	(0.02)	n/a	n/a	(0.56)	(0.29)	n/a	n/a	(0.26)	n/a	n/a

1088

1089

1090

1091 Table 1 b) The mean average (and standard deviation) for nitrate and carbonate data in winter (jan-mar), spring (apr-jun), summer (jul-sep) and
 1092 autumn (oct-dec) for each of the 9 ecohydrographic regions (numbered 1-9). Where insufficient samples exist, n/a has been used.

	Nitrate ($\mu\text{mol kg}^{-1}$)				DIC ($\mu\text{mol kg}^{-1}$)				TA ($\mu\text{mol kg}^{-1}$)				pH				pCO ₂ (μatm)			
	jan-mar	apr-jun	jul-sep	oct-dec	jan-mar	apr-jun	jul-sep	oct-dec	jan-mar	apr-jun	jul-sep	oct-dec	jan-mar	apr-jun	jul-sep	oct-dec	jan-mar	apr-jun	jul-sep	oct-dec
1	7.40	0.51	0.33	5.42	2133.27	2033.72	2063.51	2110.95	2309.71	2275.17	2291.11	2294.62	8.18	8.19	8.15	8.09	351.51	331.07	362.89	427.1
	(1.52)	(1.42)	(0.56)	(0.01)	(23.38)	(31.65)	(17.24)	(0.45)	(29.42)	(28.38)	(19.02)	(7.21)	(0.15)	(0.06)	(0.04)	(0.01)	(81.80)	(52.03)	(73.54)	(8.7)
2	4.60	1.11	0.66	6.10	2147.12	2097.67	2110.98	2144.89	2319.90	2314.85	2316.10	2331.90	8.12	8.15	8.05	8.06	382.05	376.22	483.40	469.1
	(3.22)	(2.70)	(1.06)	(7.39)	(44.05)	(18.89)	(37.72)	(24.54)	(31.15)	(29.59)	(42.68)	(32.12)	(0.03)	(0.07)	(0.10)	(0.01)	(31.20)	(58.66)	(79.58)	(11.1)
3	9.56	4.13	3.77	3.45	2133.52	2102.09	2089.84	2102.80	2326.21	2341.57	2316.24	2323.77	8.13	8.19	8.09	8.10	377.89	333.08	452.43	436.1
	(3.51)	(10.42)	(9.91)	(3.24)	(8.08)	(36.38)	(14.69)	(10.39)	(14.26)	(26.17)	(12.97)	(10.25)	(0.02)	(0.06)	(0.02)	(0.04)	(19.73)	(54.69)	(29.21)	(48.1)
4	6.55	2.05	0.49	3.37	2140.49	2111.78	2086.91	2116.19	2332.68	2333.32	2335.20	2337.16	8.12	8.17	8.14	8.12	388.10	354.57	389.88	405.1
	(3.69)	(2.44)	(2.28)	(4.06)	(7.93)	(23.78)	(18.09)	(21.57)	(9.60)	(10.09)	(14.97)	(16.05)	(0.01)	(0.03)	(0.04)	(0.04)	(13.26)	(31.18)	(49.11)	(44.1)
5	9.86	3.94	1.03	5.27	2143.20	2095.01	2076.72	2110.78	2298.23	2294.04	2293.79	2305.37	8.07	8.14	8.12	8.08	435.29	364.82	409.35	446.1
	(6.09)	(3.86)	(1.25)	(4.54)	(18.26)	(52.36)	(25.23)	(12.83)	(26.64)	(30.14)	(12.89)	(10.68)	(0.04)	(0.10)	(0.05)	(0.03)	(40.78)	(62.10)	(54.79)	(28.1)
6	6.31	0.99	1.94	0.00	2129.04	2065.03	2090.22	n/a	2287.09	2294.17	2286.60	n/a	8.06	8.18	8.11	n/a	452.97	333.27	402.89	n/a
	(0.99)	(1.50)	(1.07)	(0.00)	(15.18)	(30.84)	(7.20)	n/a	(10.89)	(10.11)	(7.31)	n/a	(0.05)	(0.05)	(0.03)	n/a	(62.04)	(43.92)	(27.48)	n/a
7	7.88	5.53	1.21	4.91	2117.70	2112.53	2090.19	2127.98	2320.55	2323.43	2301.07	2316.16	8.16	8.17	8.11	8.10	347.37	342.94	411.17	418.1
	(3.37)	(4.11)	(1.27)	(0.64)	(47.20)	(30.49)	(15.82)	(27.17)	(31.78)	(14.33)	(8.49)	(26.90)	(0.05)	(0.04)	(0.04)	(0.02)	(51.67)	(29.78)	(41.43)	(19.1)
8	10.23	6.71	0.59	n/a	2138.65	2129.34	2089.56	n/a	2332.34	2335.43	2329.87	n/a	8.12	8.15	8.15	n/a	386.80	369.86	372.79	n/a
	n/a	(2.99)	(1.00)	n/a	(2.94)	(16.17)	(11.36)	n/a	(8.47)	(6.30)	(17.18)	n/a	n/a	(0.03)	(0.03)	n/a	n/a	(24.80)	(32.84)	n/a
9	n/a	0.67	0.14	n/a	n/a	2070.94	2060.83	n/a	n/a	2298.60	2294.63	n/a	n/a	8.19	8.16	n/a	n/a	325.05	355.18	n/a
	n/a	(0.91)	n/a	n/a	n/a	(0.13)	(12.05)	n/a	n/a	(35.53)	(0.06)	n/a	n/a	(0.03)	(0.04)	n/a	n/a	(12.54)	(38.98)	n/a

2561
2562
2563
2564 1095

2565
2566
2567
2568
2569
2570
2571
2572
2573
2574
2575
2576
2577
2578
2579
2580
2581
2582
2583
2584
2585
2586
2587
2588
2589
2590
2591
2592
2593
2594
2595
2596
2597
2598
2599
2600
2601
2602
2603
2604
2605
2606
2607
2608
2609
2610
2611
2612
2613
2614
2615
2616
2617
2618
2619